



Histogenesis and reserve dynamics during the maintenance of dormancy and germination in seeds of the basal palm *Mauritiella armata*

Patrícia Pereira Fonseca¹ · Hellen Cássia Mazzottini-dos-Santos¹ · Islaine Franciely Pinheiro de Azevedo¹ · Yule Roberta Ferreira Nunes¹ · Leonardo Monteiro Ribeiro¹ 

Received: 23 August 2023 / Accepted: 19 October 2023 / Published online: 14 November 2023
© The Author(s), under exclusive licence to Springer-Verlag GmbH Austria, part of Springer Nature 2023

Abstract

The germination and post-seminal development of Arecaceae are notably complex due to the microscopic dimensions of the embryonic axis, the occurrence of dormancy, and the diversity of reserve compounds. In-depth information on this subject is still limited, especially in terms of the basal sub-family Calamoideae. *Mauritiella armata* is widely distributed in the Amazon region and is considered a key species in flooded ecosystems (*veredas*) in the Cerrado biome. We sought to describe histogenesis and reserve compound dynamics during the germination of *M. armata*, as well as the changes in incubated seeds over time. Seeds with their operculum removed (the structure that limits embryonic growth) were evaluated during germination using standard methods of histology, histochemistry, and electron microscopy. Evaluations were also performed on intact seeds incubated for 180 days. The embryos show characteristics associated with recalcitrant seeds of Arecaceae: a high water content (>80%), differentiated vessel elements, and reduced lipid reserves. Both the embryo and endosperm store abundant reserves of proteins, neutral carbohydrates, and pectins. The completion of germination involves cell divisions and expansions in specific regions of the embryo, in addition to the mobilization of embryonic and endospermic reserves through symplastic and apoplastic flows. Intact seeds show dormancy (not germinating for 180 days), but exhibit continuous development associated with cell growth, differentiation, and reserve mobilization. The anatomical and histochemical characters of *M. armata* seeds indicate an association between recalcitrance and dormancy related to the species' adaptation to flooded environments.

Keywords Embryo anatomy · Histochemistry · Palm embryo · Reserve mobilization · Seedling development

Introduction

Germination and post-seminal development are the most critical stages of a plant's life cycle (Bewley et al. 2013). During these phases, there is a transition from a condition of low metabolism to one of intense activity, and from a condition of relative protection inside the seed to exposure to the external environment while still in an incipient phase of development (Baskin and Baskin 2014a; Ribeiro et al. 2015).

These processes are remarkably complex in palms, which are widely distributed in tropical and subtropical regions, and the group shows a wide diversity of diaspore and seedling structures and sophisticated adaptive strategies (Orozco-Segovia et al. 2003; Souza et al. 2016; Moura et al. 2019; Visscher et al. 2020). Detailed studies of palm germination and seedling development have been largely concentrated in species of the Arecoideae subfamily because of economic interests, with few in-depth studies of representatives of the basal clades of Arecaceae, especially Calamoideae (Orozco-Segovia et al. 2003; Dransfield et al. 2008; Baskin e Baskin 2014a; Silva et al. 2014). The generation of more information concerning those basal clades will be important to broadening our understanding of the evolutionary history of palms and for developing efficient propagation technologies.

Germination is the resumption of embryo development after any period of quiescence (or dormancy) and involves a

Handling Editor: Peter Nick.

✉ Leonardo Monteiro Ribeiro
leomrib@hotmail.com

¹ Departamento de Biologia Geral, Universidade Estadual de Montes Claros, Montes Claros, Minas Gerais 39401-089, Brazil

series of structural and metabolic changes resulting in post-seminal development (Donohue et al. 2010; Bewley et al. 2013; Visscher et al. 2020). Palm seeds have complex anatomies and linear embryos; the embryonic axis has microscopic dimensions and is inserted within the cotyledonary petiole (Mazzottini-dos-Santos et al. 2018). Germination in Arecaceae is only completed with the displacement of the operculum (the tissues adjacent to the embryo) and the protrusion of the cotyledonary petiole, a pattern that differs from most Angiosperm species (Carvalho et al. 2015). Many species of palm trees demonstrate dormancy—the inability of the seed to germinate even under favorable environmental conditions—which is related to the low growth capacity of the embryo (Orozco-Segovia et al. 2003; Baskin and Baskin 2014b; Silva et al. 2014). The causes and classifications of dormancy in Arecaceae have not yet been fully defined (Baskin and Baskin 2014a, 2021), so that studies of the roles of seed structures in controlling germination can increase understanding of the reproduction of this important plant group (Ribeiro et al. 2015; Moura et al. 2019).

The establishment of palm seedlings requires the development of a wide variety of tissues and specialized structures dependent on the mobilization of abundant endosperm reserves (Henderson 2006; Souza et al. 2016; Dias et al. 2020). There is considerable morphological and anatomical diversity among Arecaceae seedlings (Souza et al. 2016; Moura et al. 2019), but little information is available concerning their structures and adaptive strategies in different environments, especially under flooding conditions (Silva et al. 2014; Moura et al. 2019; Dias et al. 2020).

Mauritiella armata (Mart.) Burret (Calamoideae), “buritirana” or “xiriri,” is widely distributed in South America in both the Amazon Forest and Cerrado biomes (Dransfield et al. 2008). The species is dioecious and occurs along streams and in swamps and seasonally flooded savannas; it is commonly associated with the palm *Mauritia flexuosa* L.f. (Smith 2015; Ávila et al. 2022, 2023). *M. armata* is considered ecologically important as it provides food for the regional fauna and helps regulate the hydrological cycles of flooded environments (“veredas”) in the Brazilian Cerrado, ecosystems that are severely threatened by anthropic pressures (Smith 2015; Ávila et al. 2022; Nunes et al. 2022). The species is also of socio-economic importance, as the mesocarp (which has nutritional and antioxidant properties) can be consumed in the form of juices, sweets, jellies, and ice cream; various parts of the plant are used in making handicrafts (Souza et al. 2022). Additionally, studies have indicated the potential use of fibers extracted from the stems of that palm as adjuvants in the production of epoxy (Souza et al. 2020). Botanical information concerning this species is still extremely limited, however, with only preliminary information being currently available concerning seed characterization (Lorenzi et al. 2010), with no detailed records focusing on its germination. As such, reproductive

studies of *M. armata* may provide subsidies for its sustainable use and conservation.

We provide here anatomical, histochemical, and ultrastructural descriptions of *M. armata* seeds throughout their germination processes to address the following questions: (i) what are the roles of cell division and cell expansion in the embryo/seedling transition? (ii) what is the cellular structure of the seed, and what are the dynamics of its reserve compounds during germination? (iii) what anatomical and histochemical changes occur in incubated seeds over time?

Materials and methods

Fruit collection and preliminary procedures

Mauritiella armata fruits were collected after natural abscission in a population growing in the Veredas do Peruçu State Park, in the municipality of Cônego Marinho, in northern Minas Gerais State, Brazil (14° 56' 13" S × 44° 37' 44" W). Only whole fruits with no signs of predation or microbial deterioration were selected. A yellowish abscission scar was considered indicative of recent abscission (Silva et al. 2014).

The pericarp was manually removed, and any seeds damaged by pathogens or insects were discarded. The seeds were sectioned, the embryos extracted, and the water contents of four replicates of 10 isolated embryos and endosperm + seminal envelopes were evaluated, considering the relationship between their fresh and dry weights after drying at 105°C for 24 h (Brasil 2009). The seeds were disinfected in 6% sodium hypochlorite for 15 min, washed in running water, treated with a fungicide (Derosal Plus® 50%), and kept in closed polypropylene bags (500 µm thick) at 20°C until used (Veloso et al. 2016). Seeds not directly used in the experiments were stored for 12 months and their viabilities subsequently evaluated by the tetrazolium test (Brasil 2009).

Preliminary tests indicated that seeds sown into polyethylene containers (17×12×6cm) in sterilized sand (moistened with distilled water to up to 80% of its retention capacity) and subsequently held in a germinator at 30°C did not germinate for 60 days (Silva et al. 2014). As these results suggested seed dormancy, the seeds were divided into two lots and subjected to additional treatments. The seeds of the first lot had the operculum (the tissues adjacent to the embryo that limit its growth) removed using a stylus—an efficient treatment for overcoming dormancy in palm seeds (Silva et al. 2014). The seeds were then sown into sand as described above. Samples were periodically removed for morphological, anatomical, and histochemical evaluations. The seeds of the second lot were sown intact, and the germination of five replicates of 10 seeds each was monitored weekly for 180 days. Those replicates were successively submitted to the same evaluations as described above.

Seed and seedling morphology

One hundred seeds with their operculum removed were observed daily for 30 days, and then every 3 days for up to 180 days. Seed and seedling morphologies were characterized according to the criteria established by Silva et al. (2014). Images of those materials were recorded using a digital camera (sx520 hs, Canon, Tokyo, Japan).

Embryo micromorphology

Five embryos in their initial condition were fixed in Karnovsky's solution (Karnovsky 1965), dehydrated in an ethanolic series, and dried to their critical point in CO₂ in a Bal-Tec apparatus (Leica Microsystems, Heidelberg, Germany). The samples were subsequently coated with a 10-nm layer of gold using a Bal-Tec-MD20 metallizer (Leica Microsystems, Heidelberg, Germany) (Robards 1978) and examined in a scanning electron microscope (Quanta 200, FEI Company, Eindhoven, Netherlands). Images were captured digitally at 12–20 kV.

Seed and seedling anatomy

Samples of the cotyledonary petiole, haustorium, endosperm, and root were obtained from cultivated seeds (without their operculum) before sowing, 3 days after sowing, and then during the phases of protrusion of the cotyledonary petiole, expansion of the ligule, and after the emission of the main root (Silva et al. 2014; Dias et al. 2020). Samples of the cotyledonary petiole, haustorium, and endosperm were also obtained from intact seeds after 180 days of incubation. Five seeds were evaluated on each occasion. The material was fixed in Karnovsky's solution (Karnovsky 1965), dehydrated in an ethanolic series, and included in 2-hydroxyethylmethacrylate (Leica®), following Paiva et al. (2011). Cross and longitudinal sections (3–5 µm thick) were obtained using a rotating microtome (HistoCore Autocut, Nussloch, Germany), stained with 0.05% toluidine blue, pH 4.7 (O'Brien et al. 1964, modified), and mounted on slides with acrylic resin (Itacril, Itaquaquecetuba, Brazil). The sections were evaluated by viewing under a photomicroscope (Zeiss Lab AI/Axion Cam ICC 3, Jena, Germany).

Histochemical evaluations

Additional sections of the same materials processed as above for anatomical analyses were stained with periodic acid and Schiff's reagent-PAS to identify neutral polysaccharides (Feder and O'Brien 1968), with choriphosphine to identify acidic polysaccharides (Weis et al. 1988), with xyloidine-Ponceau (Vidal 1970) to identify proteins, and with neutral red to identify lipophilic compounds (Kirk 1970).

Ultrastructural evaluation

The protoderm and ground meristem of the cotyledonary petioles of embryos obtained from five intact seeds in the initial condition, and then after 180 days of incubation, were evaluated. The samples were fixed in Karnovsky's solution (Karnovsky 1965) for 24 h, post-fixed in 1% osmium tetroxide (0.1 M phosphate buffer), dehydrated in an acetone series, infiltrated in Araldite resin (Robards 1978; Roland 1978), and sectioned using a UCB ultramicrotome (Leica Microsystems, Heidelberg, Germany). The fragments were counterstained with uraline acetate solution (Watson 1958) and lead citrate (Reynolds 1963). Images were obtained digitally in a transmission electron microscope (Tecnai G2-20-SuperTwin, FEI Company, Eindhoven, Netherlands) at 200 kV.

Results

The water content of newly dispersed seeds and of isolated embryos was 46.8% and 81.0% respectively. Eighty-two percent of the seeds were viable; that value decreased to 58% after 12 months of storage under humid conditions.

Seed and seedling morphology

Mauritiella armata seeds are oval, with a thin, dark brown seed coat (Fig. 1A). The endosperm is abundant, rigid, and whitish. The embryo is linear, is inserted into the micropylar region, and has a conical shape with two distinct regions: the cotyledonary petiole (yellowish and more dilated proximally) and the haustorium (whitish, with its distal portion more elongated and narrow). The operculum is disc-shaped in the micropylar region, and is composed of the opercular seed coat and the micropylar endosperm; it protects the embryo but also restricts its growth. The operculum is displaced under natural conditions when germination has been completed; this occurs through the rupture of a zone of weakness in the endosperm.

The germination of seeds with their operculum removed occurred approximately 5 days after sowing, and was associated with embryo elongation and the emission of the cotyledonary petiole (Fig. 1B). The ligule (the lateral portion of the cotyledonary petiole) then expands and forms a protuberance—the germinative bud. The main root emerged from the expanded ligule 15 days after sowing (Fig. 1C). In this phase, the haustorium showed significant growth, indicating an intense mobilization of endosperm reserves, with the formation of a digestion zone. The first tubular-shaped leaf sheath was emitted 17 days after sowing (in a region of the germinative bud, opposite the root), concomitant with the emission of adventitious roots from the ligule (Fig. 1D). The second leaf sheath is emitted internally (in

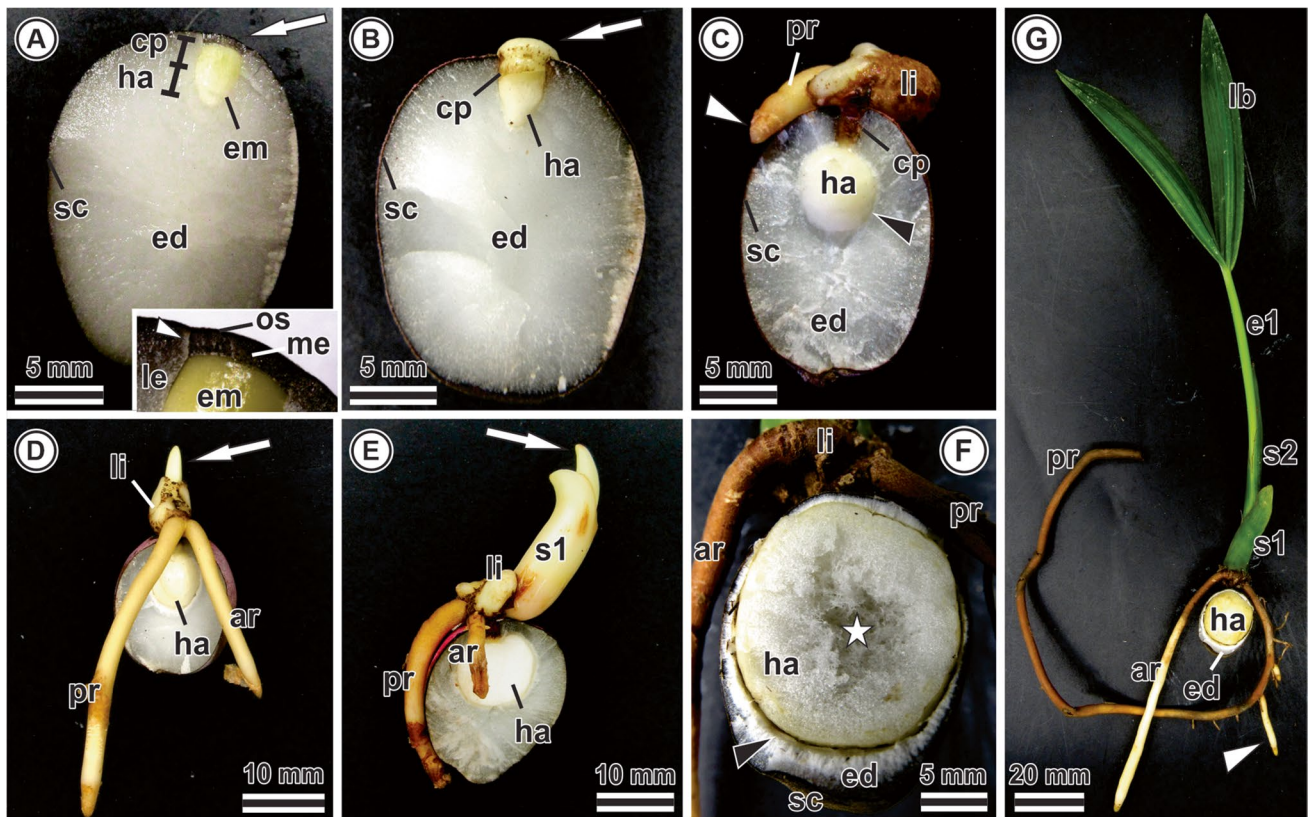


Fig. 1 *Mauritiella armata* seed and seedling morphology. Seeds sectioned lengthwise. Intact seeds (A); seeds sown after the operculum has been mechanically removed (B–G). Seed in initial condition, showing embryo adjacent to operculum (arrow); detail of the micropylar region in the lower right corner, highlighting the weakness zone (arrowhead) (A). Cotyledonary petiole (arrow) protrusion phase (B). Main root protrusion phase; root with developed cap (white arrowhead) and haustorium with significant growth showing the digestion zone (black arrowhead) (C). Emission phases of the first (D) and second (E) leaf sheaths (white arrows), with the presence of adventi-

tious roots. Seed during the emission phase of the first eophyll, showing the final consumption of endosperm reserves and increase in the thickness of the digestion zone (black arrowhead), highlighting the cavity formed inside the haustorium (asterisk) (F). Seed and seedling, after 150 days of sowing, showing the developed structures; highlight for the lateral roots (arrowhead) (G). ar, adventitious root; cp, cotyledonary petiole; e1, first eophyll; ed, endosperm; em, embryo; ha, haustorium; lb, leaf blade; le, lateral endosperm; li, ligule; me, micropylar endosperm; os, opercular seed coat; pr, main root; sc, seed coat; s1, first leaf sheath; s2, second leaf sheath

relation to the first), approximately 30 days after sowing (Fig. 1E). The first eophyll (photosynthetic leaf) was emitted after approximately 55 days. At 150 days after sowing, the seedlings had an eophyll with expanded limbs, as well as a root system composed of a main root and numerous lateral and adventitious roots (Fig. 1G). The haustorium grew to occupy most of the seminal cavity and had a spongy aspect, with the formation of a large cavity in the central region (Fig. 1F–G). The digestion zone became even more evident and had a peripheral disposition, indicating the final phase of endosperm reserve mobilization (Fig. 1F).

Embryo micromorphology

The transition region between the cotyledonary petiole and haustorium of *M. armata* is well delimited (Fig. 2A). The petiole has a flat surface, with an opening that corresponds

to the cotyledonary cleft (disposed laterally), through which the aerial portion is emitted (Fig. 2B); endosperm remnants are observed in this region (Fig. 2C). At the proximal end of the petiole, it is possible to observe the scar of the persistent suspensor, which holds the embryo in the micropylar endosperm and is ruptured when it is extracted (Fig. 2A). The conical haustorium has villi on its surface (Fig. 2A, D–E) and there are projections on the protodermal cell walls (Fig. 2D) that increase the absorptive surfaces.

Seed and seedling anatomy

The seed coat is formed by cells with thick, lignified walls that accumulate phenolic compounds (Fig. 3A–B). Between the lateral and micropylar endosperms, there is a zone of weakness formed by longitudinally elongated cells that favor

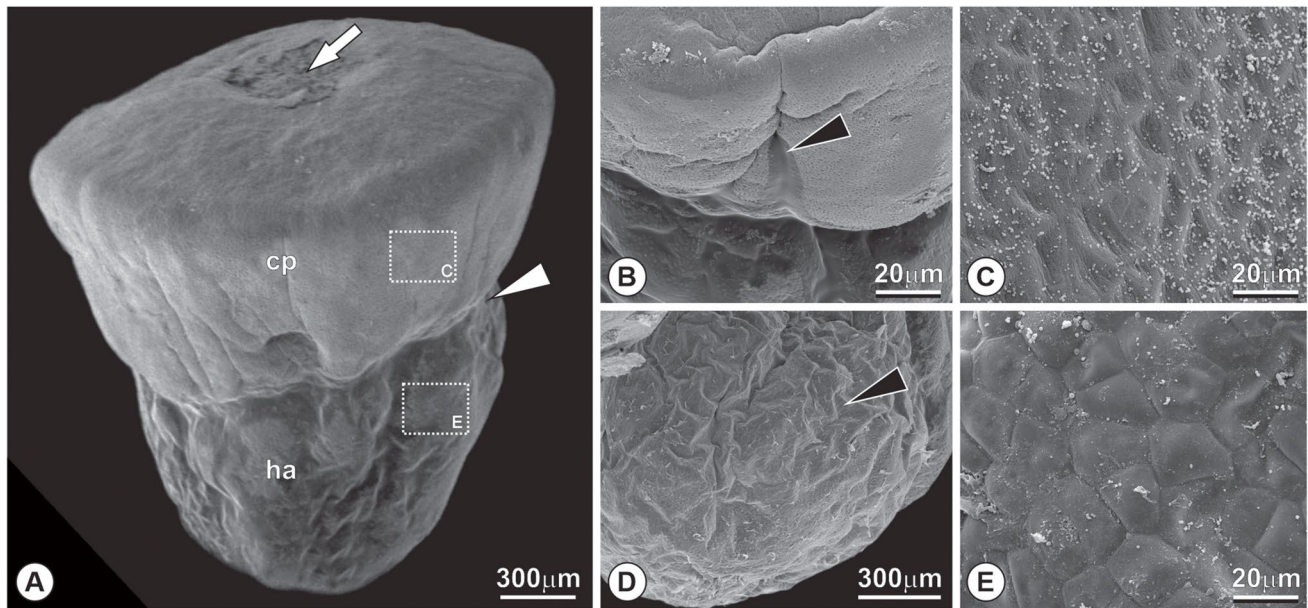


Fig. 2 Micromorphology of the *Mauritiella armata* embryo. Embryo, showing the cotyledonary petiole and the haustorium and the transition region between the structures (arrowhead) (A); scar left by the rupture of the suspensory (white arrow). Cotyledonary cleft (arrow-

head) (B). Surface of the cotyledonary petiole, with endosperm residues (C). Surface of the haustorium, with shallow villi (arrowhead) and cells with small projections from the wall (D–E). cp, cotyledonary petiole; ha, haustorium

the displacement of the operculum during the conclusion of germination (Fig. 3B). The embryonic axis is inserted within the cotyledonary petiole and is positioned obliquely in relation to the longitudinal axis of the embryo; the plumule is disposed laterally towards the cotyledonary cleft, while the hypocotyl-radicle axis is projected towards the micropylar region (Fig. 3A, C). The plumule is composed of two leaf sheaths surrounding the shoot promeristem (Fig. 3C); it is covered by the lateral portion of the cotyledonary petiole, the ligule (Fig. 3A). The hypocotyl-radicle axis is evident, but does not have a differentiated protoderm; it is contiguous to the fundamental meristem of the cotyledonary petiole and is formed by small peripheral procambial cells as well as elongated and vacuolated cells, positioned centrally (Fig. 3C). The protoderm delimits the entire cotyledon, being uniseriate and composed of cuboidal and compactly arranged cells. There is a deep invagination of the protoderm adjacent to the plumule, forming an opening to the external environment—the cotyledonary cleft (Fig. 3A, F). Procambial strands depart from the embryo axis in the region of the cotyledonary node, forming a sympodium, towards the haustorium (Fig. 3A). A ground meristem is abundant throughout the cotyledon, consisting of thin-walled cells with large vacuoles with mucilaginous accumulations (Fig. 3E, G). Differentiated vessel elements occur near the cotyledonary node (Fig. 3D). The haustorium has small invaginations in the protodermis (Fig. 3A, G) and is permeated by peripherally disposed procambial cords (Fig. 3A, G–H). The endosperm

is formed of cells with thick walls and voluminous vacuoles that store mucilage (Fig. 3H). There is a thin layer of collapsed cells in the endosperm adjacent to the haustorium that is indicative of reserve mobilization during the pre-dispersal phase (Fig. 3H).

Alterations of the embryo were evident 3 days after sowing seeds without their operculum, including the elongation of the embryo axis and the mobilization of reserves in the cotyledonary petiole (Fig. 4A–C). Cells in the medullary region of the hypocotyl-radicle axis became more elongated (Fig. 4B), and the plumule showed a slight expansion (Fig. 4C). Cell divisions could be observed in the ground meristem, in the region opposite the ligule (Fig. 4D). Cell expansion occurred in the ground meristem at the proximal end of the cotyledonary petiole (Fig. 4E), and a proliferation of procambial cords in the middle region of the petiole was quite notable (Fig. 4F). The beginning of endosperm reserve mobilization was evident, associated with the dilation of the primary pit fields that indicated symplastic translocation (Fig. 4G–H). Concomitantly, granular material accumulated along the periphery of the haustorium.

During the phase of cotyledonary petiole protrusion, the tissues of the primary structure of the seedling demonstrated signs of differentiation. The formation of the germinative bud was associated with cell divisions and cell expansion (Fig. 5A). Differentiation of the epidermis and parenchyma was evident throughout the cotyledon (Fig. 5B–I). Idioblasts

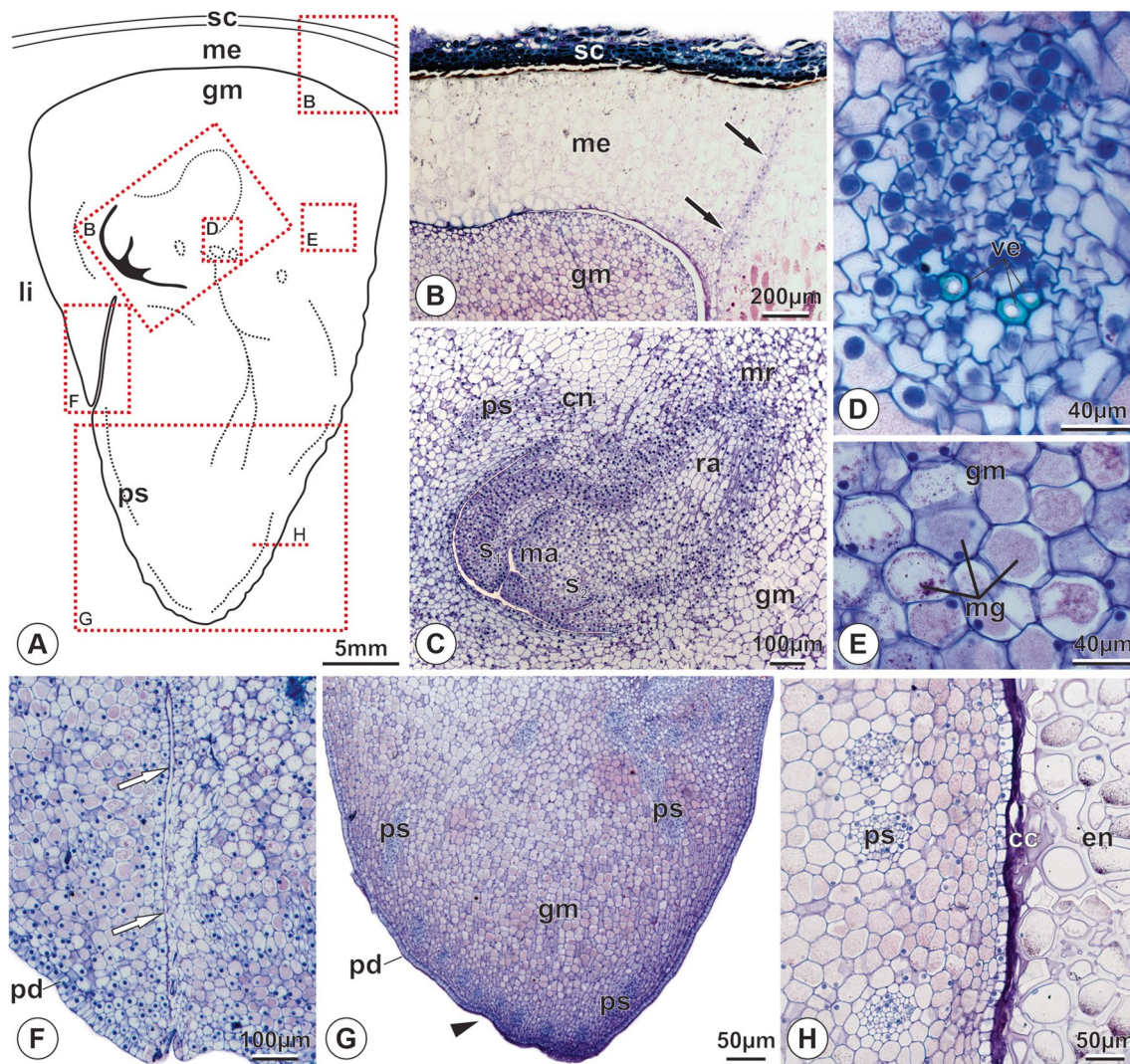


Fig. 3 Longitudinal (B–G) and cross (H) sections of *Mauritiella armata* seed. Scheme of the embryo and the micropylar region, highlighting the embryo axis and distribution of the procambial strands (black dotted lines); red dotted lines represent regions shown in B–H (A). Micropylar region showing the opercular seed coat, micropylar endosperm, and zone of weakness (arrows) (B). Embryo axis showing the plumule and the hypocotyl-radicle axis (C). Procambial strand with differentiated vessel elements (D). Ground meristem cells of the cotyledonary petiole, with accumulation of granular material (E).

Peripheral region of the cotyledon showing the cotyledonary cleft (arrows) (F). Haustorium, highlighting invaginations in the protodermis (arrowhead) (G). Haustorium/endosperm interface (H). cc, layer of collapsed cells; cn, cotyledonary node; en, endosperm; gm, ground meristem; li, ligule; ma, shoot apical meristem; me, micropylar endosperm; mg, granular material; mr, meristematic region; pd, protoderm; ps, procambial strands; ra, hypocotyl-radicle axis; sc, seed coat; s₁, first leaf sheath; s₂, seconde leaf sheath; ve, vessel element

with accumulations of phenolic compounds became differentiated in the ligule, the apex of the root, and in the proximal region of the cotyledonary petiole adjacent to the epidermis (Fig. 5B–D). The expressive growth of the plumule, as a result of cell divisions and expansion, forced a partial opening of the cotyledonary cleft (Fig. 5B). Cells in the medullary region of the root became even more elongated, and meristematic activity was notable in the region adjacent to the root apex (Fig. 5C); the cells in the proximal end of the cotyledonary petiole collapsed due to the pressure generated by this meristematic activity. The cells in the

proximal region of the cotyledonary petiole were observed to be dividing and expanding intensely (Fig. 5D). Rows of raphidic idioblasts were conspicuous in this region. Cell divisions were also observed in the ligule (Fig. 5E). The parenchyma and epidermal cells in the distal region of the cotyledonary petiole became more elongated as compared to other regions, highlighting their roles in seedling protrusion (Fig. 5G). Differentiating vascular bundles could be identified along the cotyledonary petiole (Fig. 5H). The mobilization of endosperm reserves intensified during this phase, with evident thickening of the layer of collapsed

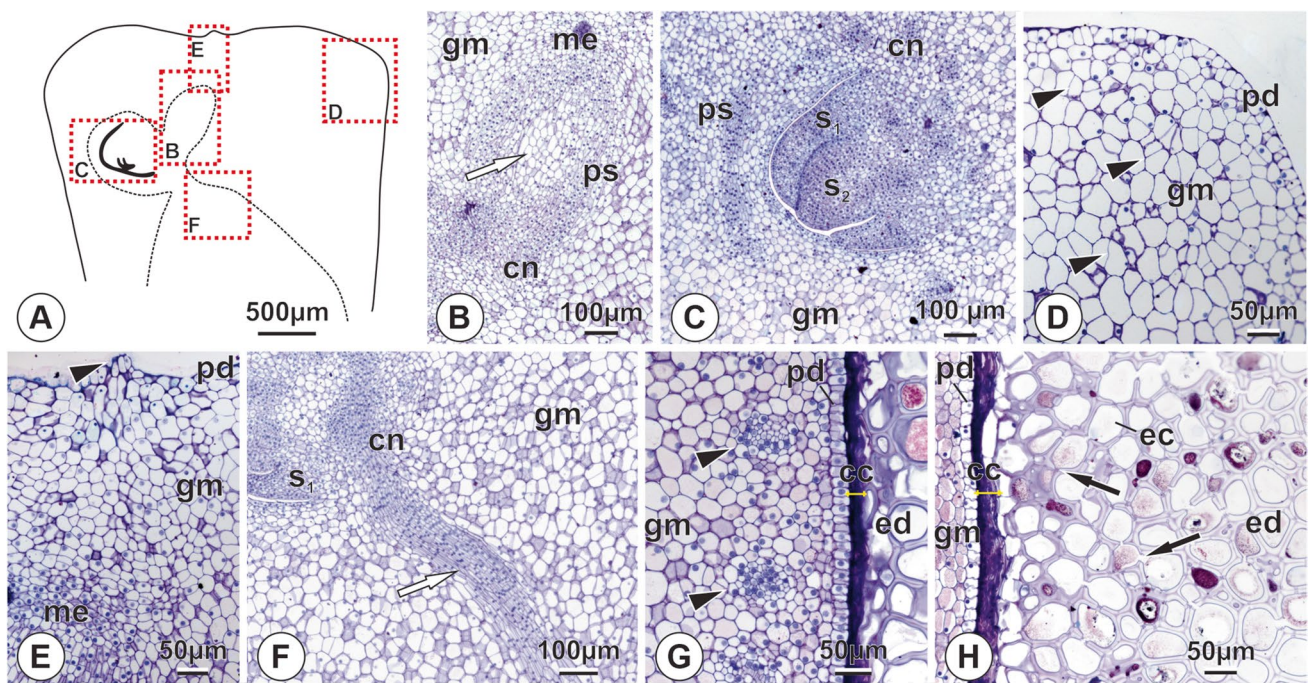


Fig. 4 Longitudinal (B–F) and cross (G–H) sections of *Mauritiella armata* seeds, whose opercula were mechanically removed, 3 days after sowing. Scheme of the cotyledonary petiole showing the procambial strands (black dotted lines); the red dotted rectangles correspond to the regions shown in B–F (A). Hypocotyl-radicle axis with expanded cells in the medullary region (arrow) (B). Plumule with first and second leaf sheath (C). Proximal region of the petiole, opposite the ligule, showing cells with evidence of recent divisions (arrowheads) (D). Extremity of the cotyledonary petiole, highlight-

ing part of the suspensor (arrowhead) (E). Procambial strand close to the cotyledonary node, with cell proliferation (arrow) (F). Haustorium, indicating the peripheral procambial strands (arrowheads) (G). Haustorium/endosperm interface, showing evidence of translocation of endosperm reserves by symplastic flow (arrows) (H). cc, layer of collapsed cells; cn, cotyledonary node; ec, empty cell; ed, endosperm; me, radicular apical meristem; gm, ground meristem; me, radicular apical meristem; pd, protoderm; ps, procambial strand; s1, first leaf sheath; s2, second leaf sheath

cells adjacent to the haustorium (Fig. 5I). Vascular bundles, with differentiated vessel elements, were also evident in the haustorium.

The ligule expansion phase was associated with intense cell divisions, expansion, and differentiation (Fig. 6A–F). The differentiation of raphidic idioblasts in the ligule and their accumulation of phenolic compounds was evident (Fig. 6B). Phenolic compounds could also be observed along the peripheries of the leaf sheaths. Meristematic activity adjacent to the root intensified; a set of those generated cells differentiated into phenolic idioblasts associated with the formation of the root cap (Fig. 6C). Phenolic compounds accumulated at the proximal end of the petiole as well as at the proximal end of the petiole (Fig. 6D). The cells in this region showed significant expansion, and the differentiation of numerous raphide idioblasts was evident. Intense cell divisions could be seen in the innermost regions of the ligule and in the distal regions of the germinative bud, occurring concomitantly with the differentiation of idioblasts containing phenolic compounds (Fig. 6E–F). The vascular bundles in the haustorium had expanded, with evident xylem differentiation, with phenolic idioblasts proliferating in the

peripheral region (Fig. 6G). Numerous intercellular spaces could be observed in the inner region of the haustorium, with the formation and differentiation of phenolic idioblasts (Fig. 6G–H).

During the root protrusion phase, there was differentiation of the first eophyll at the shoot apex and significant expansion of the plumule (Fig. 7A–B). The root showed a well-developed cap, with accumulations of phenolic compounds (Fig. 7C). The parenchyma cells of the cortical region were elongated, with rows of large idioblasts containing raphides forming large spaces within the root. An intense proliferation of idioblasts containing phenolics was seen in the inner region of the root, being most prominent adjacent to the vascular cylinder; intense vascularization and meristematic activity were evident at the root-shoot interface (Fig. 7D). The significant increase in the thickness of the collapsed endosperm cell layer in the haustorium indicated intense reserve mobilization (Fig. 7E), and the formation of an aerenchyma could be observed in the innermost region (Fig. 7E–F).

Intact seeds incubated for 180 days did not germinate. However, some anatomical characteristics indicated

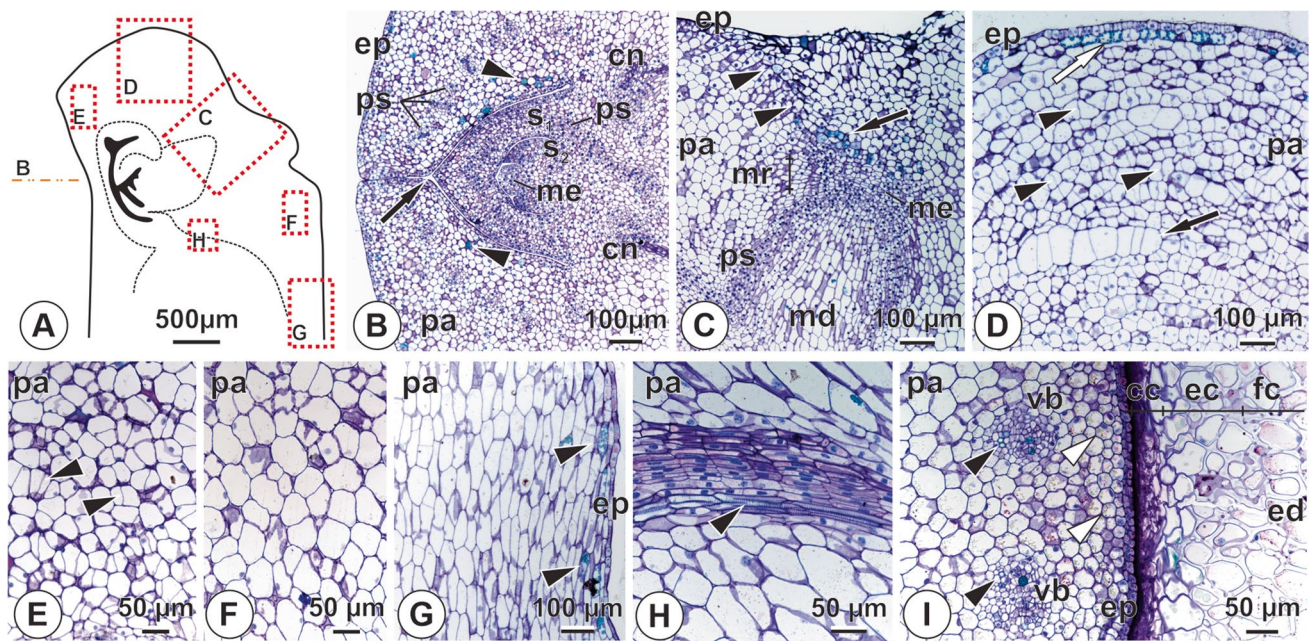


Fig. 5 Cross (B, I) and longitudinal (C–H) sections of seeds and seedlings of *Mauritiella armata* in the cotyledonary petiole protrusion phase. Scheme of the cotyledonary petiole, showing the procambial strands/vascular bundles (black dotted lines); red dotted lines represent regions shown in B–H (A). Plumula region, highlighting phenolic idioblasts (arrowheads) and opening in the cotyledonary cleft (arrow) (B). Proximal region of the cotyledonary petiole, showing the growing root, the accumulation of phenolic compounds (arrow) and the region of compression of the cells at the end of the petiole (arrowheads) (C). Region opposite the ligule, showing accumulation of phenolic compounds (white arrow), idioblasts containing raphids (black arrow) and cells with evidence of divisions (black arrowheads) (D). Ligule, showing cells with evidence of divisions (arrowheads) (E). Expanded parenchyma cells in the region oppo-

site the ligule (F). Distal region of the cotyledonary petiole, showing elongated parenchyma cells and accumulation of phenolic compounds close to the epidermis (arrowheads) (G). Vascular bundle with differentiated vessel elements (arrowhead) (H). Haustorium/endosperm interface highlighting vascular bundles with differentiated vessel elements (black arrowheads) and accumulation of granular material (white arrowheads) in the haustorium, expansion of the collapsed cell layer and gradient of reserve mobilization in the endosperm (I). cc, layer of collapsed cells; cn, cotyledonary node; ec, empty cell; ed, endosperm; ep, epidermis; fc, full cell; md, medullary region of the root; me, shoot meristem; mr, meristematic region; pa, parenchyma; ps, procambial strands; s1, first leaf sheath; s2, second leaf sheath; vb, vascular bundle

a continuous development typical of recalcitrant seeds. Reserve consumption in the cotyledonary petiole was notable, with some cell divisions being evident at the proximal end (Fig. 8A–B). A symplastic flow of reserves in the endosperm could be identified (Fig. 8C), and slight accumulations of mucilaginous substances were observed in the haustorium.

Seed and seedling histochemistry

In their initial condition before sowing, the cells of the ground meristem and procambial strands of the cotyledonary petiole (Fig. 9A–C), as well as the haustorium (Fig. 9D, F), had abundant protein reserves stored in large vacuoles; similar reserves were also observed in the endosperm (Fig. 9D–E). Evidence of protein mobilization in the pre-dispersal phase was seen in the cotyledonary petiole (Fig. 9A, C) and endosperm cells (Fig. 9E); extravasation of protein compounds into the intercellular spaces was observed in the haustorium, indicating apoplastic flow (Fig. 9F).

After 3 days of cultivation of the seeds without their operculum, protein reserve mobilization intensified in the cotyledonary petiole and endosperm (Fig. 9G–K), and the proteins in the proximal end of the petiole (region adjacent to the suspensor) were largely mobilized (Fig. 9H). A digestion gradient was evident in the endosperm near the haustorium, with symplastic flows of reserve degradation products (Fig. 9J–K). While proteins were not very evident in haustorial protoderm cells in the initial condition, they now showed accumulations of these compounds (Fig. 9J); the cells located in the central region, however, did not differ from their initial condition (Fig. 9L). During the cotyledonary petiole protrusion phase, the petiole protein reserves were mostly mobilized (Fig. 9M). The endosperm evidenced a significant increase in protein reserve mobilization as compared to the previous phases (Fig. 9N), with the proteins now being concentrated in regions close to the primary pit fields as is characteristic of symplastic flow. Accumulations of protein compounds in the epidermis and subepidermal layer of the haustorium were evident, as well as the

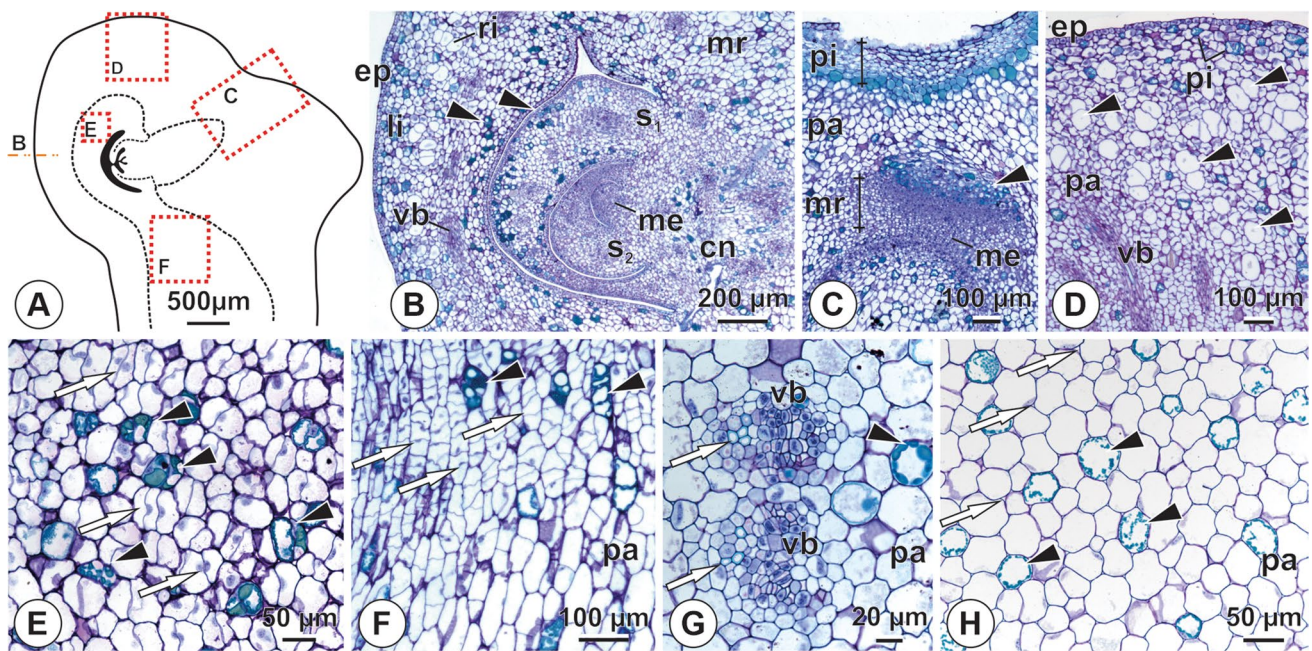


Fig. 6 Longitudinal (B–F) and cross (G–H) sections of seeds and seedlings of *Mauritiella armata*, during the ligule expansion phase. Scheme of the cotyledonary petiole, showing the embryo axis and vascularization (black dotted lines); red dotted lines correspond to regions shown in B–F (A). Plumule region highlighting phenolic idioblasts (arrowheads) (B). Proximal region of the petiole, showing the root apex and the accumulation of phenolics at the end and in the root cap formation region (arrowhead) (C). Petiole end with numerous raphidic idioblasts (black arrowhead) (D). Region adjacent to the shoot apex, showing cells with evidence of intense division (white arrows) and idioblasts containing phenolics (arrowheads) (E). Dis-

tal region of the petiole, showing elongated parenchyma cells, cells with evidence of divisions (white arrows), and idioblasts with phenolic accumulation (arrowheads) (F). Peripheral region of the haustorium, with vascular bundles with differentiated vessel elements (arrows) and idioblasts containing phenolics (black arrowhead) (G). Internal region of the haustorium, highlighting intercellular spaces (arrows) and accumulation of phenolic compounds (arrowheads) (H). cn, cotyledonary node; ep, epidermis; li, ligule; me, apical meristem; mr, meristematic region; pa, parenchyma; pi, phenolic idioblasts; ri, raphidic idioblast; s1, first leaf sheath; s2, second leaf sheath; vb, vascular bundle

beginning of their mobilization in the innermost regions of the parenchyma, with those cells showing flocculated protein remnants (Fig. 9O). In the ligule expansion phase, protein reserves were observed to have been partially mobilized in the shoot apex region (Fig. 9P). The protein contents of the endosperm cells adjacent to the haustorium had been mostly mobilized, leaving flocculated reserve remnants (Fig. 9Q). Protein reserve mobilization was also evident in the parenchyma cells of the haustorium (Fig. 9R). In the root, protein depositions were observed in the peripheral region of the root cap and in the medullary region (Fig. 9S–U).

In their initial condition, the cells of the cotyledonary petiole held an abundance of neutral polysaccharides (Fig. 10A–C), mostly in the plumule region, with evidence of their partial mobilization in some cells (Fig. 10B–C). Neutral polysaccharides were concentrated in the thick cell walls and, to a lesser extent, in the vacuoles of endosperm cells (Fig. 10D). The same distribution patterns of these compounds were observed in all of the haustorium cell types (Fig. 10E–F).

After 3 days of cultivation of seeds without an operculum, there was expressive mobilization of neutral polysaccharides

in the cotyledonary petiole, with the formation of small transitory starch grains (Fig. 10G). Evidence of neutral polysaccharide mobilization was also observed in the endosperm cell walls (Fig. 10H), but no alterations were observed in the haustorium in relation to the initial condition (Fig. 10I). During the petiole protrusion phase, the neutral polysaccharide reserves of the cotyledonary petiole were mostly consumed, leaving only flocculated remnants (Fig. 10J–K). The beginning of the mobilization of haustorial reserves was observed mainly in the parenchyma cells adjacent to the vascular bundles, where starch grain accumulations were evident (Fig. 10L). The intensification of polysaccharide accumulation in the endosperm cell walls indicated apoplastic reserve flow. Starch deposition increased in the plumule and haustorium region during the ligule expansion phase (Fig. 10M, O). There were reductions of polysaccharides in the endosperm vacuoles and increases in their concentrations in the cell walls and in the collapsed cell layers (Fig. 10N). Neutral polysaccharides were observed in root cell walls and were abundant in the root cap (Fig. 10P–R). Starch grains were distributed throughout the root, but were more concentrated in the meristematic region.

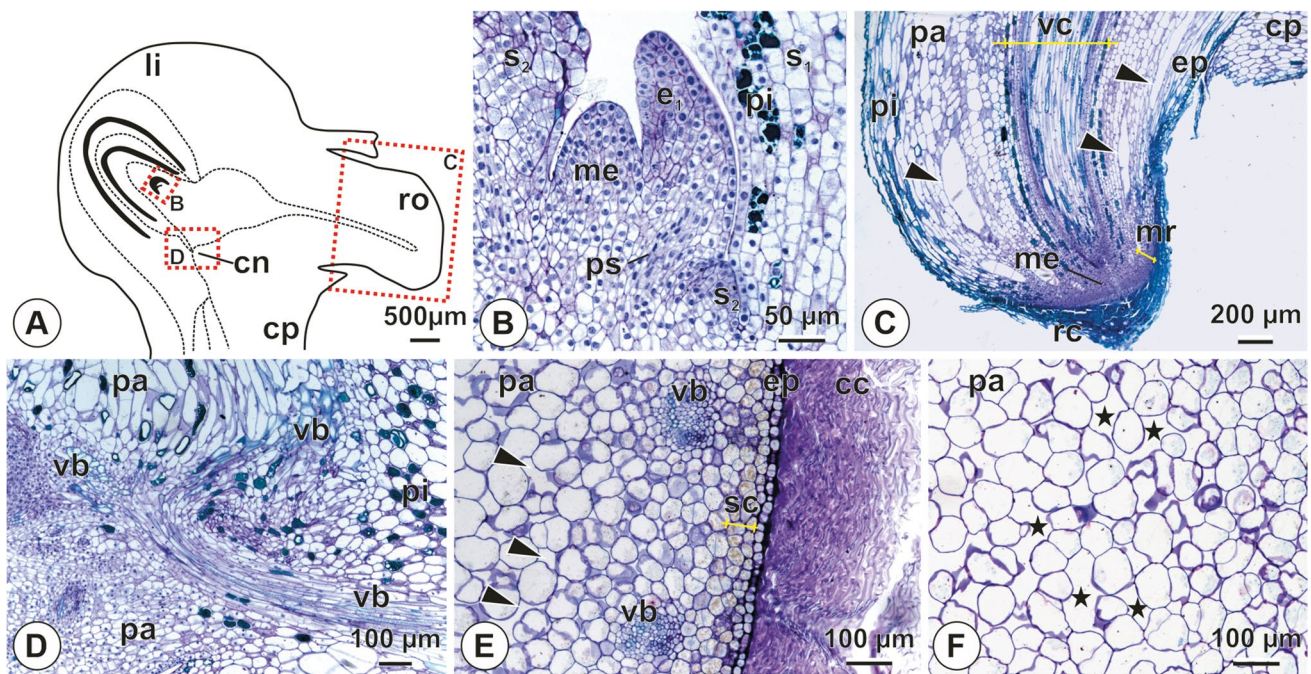


Fig. 7 Longitudinal (B–D) and cross (E–F) sections of seeds and seedlings of *Mauritiella armata* during root protrusion phase. Scheme of the germinative bud, showing the vegetative and the vascularization (black dotted lines); red dotted rectangles indicate the regions shown in B–D. Stem apex, with shoot meristem, leaf sheaths and first eophyll (B). Main root, highlighting the large spaces formed by the fusion of raphidic idioblasts (arrowheads) (C). Shoot/root interface with intense vascularization and meristematic activity (D). Haustorium/endosperm interface, showing accumulation of granular material in the subepidermal layers and intercellular spaces (arrow-

heads); emphasis on the highly enlarged layer of collapsed cells (E). Internal region of the haustorium showing the formation of aerenchyma by the fusion of intercellular spaces (asterisks) (F). cc, collapsed cell layers; cn, cotyledonary node; cp, cotyledonary petiole; e1, first eophyll; ep, epidermis; li, ligule; me, apical meristem; mr, meristematic region; pa, parenchyma; pi, phenolic idioblasts; ps, procambial strands; rc, root cap; ro, root; s1, first leaf sheath; s2, second leaf sheath; sc, subepidermal layer; vb, vascular bundle; vc, vascular cylinder

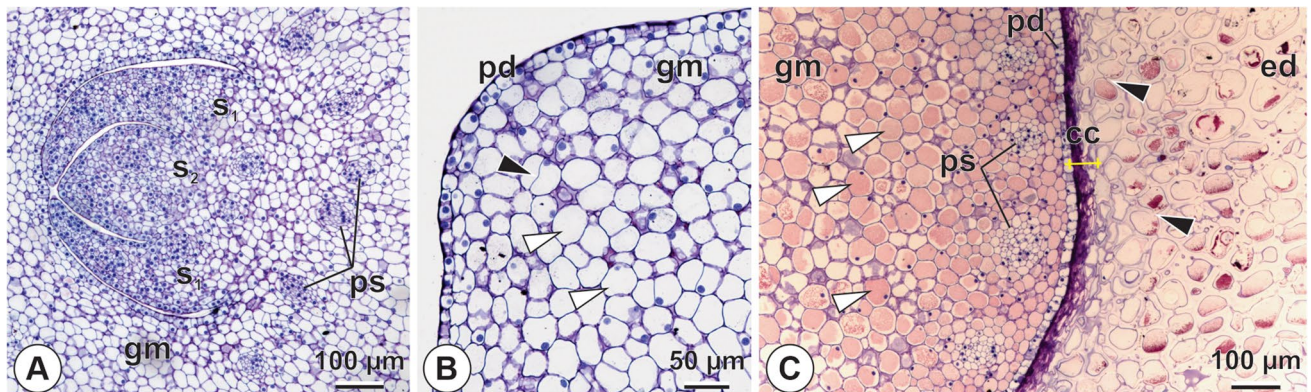


Fig. 8 Longitudinal (A–B) and cross (C)-sections of dormant seeds of *Mauritiella armata*, 180 days after sowing. Plume with cells showing internal expansion (A). Proximal region of the cotyledonary petiole with vacuolated ground meristem cells without accumulation of reserves (white arrowheads) and with evidence of division (black arrowhead)

(B). Haustorium/endosperm interface showing mucilage accumulation in the haustorium (white arrowheads) and translocation of endospermic reserves (black arrowheads) (C). cc, collapsed cell layers; ed, endosperm; gm, ground meristem; pd, protoderm; ps, procambial strands; s1, first leaf sheath; s2, second leaf sheath

In the initial condition, pectins were observed in the cell walls of the cotyledonary petiole as well as in the middle lamella and in the protoderm and ground meristem

(Fig. 11A). In the endosperm, pectins were likewise found in the middle lamella, inner cell wall, and vacuole, with evidence of their mobilization through symplastic flow

(Fig. 11B). The occurrence of pectins in the haustorium was limited to the protoderm cell walls (Fig. 11C).

Both the cotyledonary petiole and haustorium showed significant pectin depositions in their cell walls and vacuoles 3 days after sowing (Fig. 11D, F). The endosperm adjacent to the haustorium also showed pectin accumulations in the middle lamella, vacuoles, cell walls, and the collapsed cell layer (Fig. 11E). Pectin deposition in the cotyledonary petiole increased considerably after its protrusion, especially in the epidermis and underlying layers, and was concentrated in the intercellular spaces, middle lamella, cell walls, periplasmic spaces, cytoplasm, and vacuoles (Fig. 11G). At this stage, pectins were being mobilized in the endosperm by symplastic flow (Fig. 11H), and in the haustorium by apoplastic flow (as was evidenced by their deposition in the intercellular spaces) (Fig. 11I). During the ligule expansion phase, the deposition of pectic substances significantly increased in all cell types of the cotyledonary petiole (Fig. 11J), epidermis, and in the subepidermal layer of the haustorium (Fig. 11K–L). Enhanced symplastic flows of endosperm pectic reserves were also notable (Fig. 11K). Pectins were only abundant in the cell walls of the median region of the root (after its protrusion) (Fig. 11M–O).

Dormant seeds, after 180 days of cultivation, showed partial mobilization of protein reserves in the cotyledonary petiole, with greater intensity in the plumule (Fig. 12 A–B); an expressive mobilization of these reserves was evident in the endosperm (Fig. 12C). No significant changes were observed in the haustorium, however, in relation to the initial condition. Neutral polysaccharides, which were initially stored in the vacuoles of the ground meristem cells of the cotyledonary petiole, were observed to have been largely mobilized (Fig. 12E–F). The reduction of neutral polysaccharides in the vacuoles of the endosperm adjacent to the haustorium, and their accumulation in the cell walls and collapsed cell layers was notable (Fig. 12G). The haustorium did not evidence any significant alteration in comparison to the initial condition. Pectic substances had become concentrated in the middle lamella, cell walls, and vacuoles of the protoderm and ground meristem of the cotyledonary petiole (Fig. 12I–J). In the endosperm, these substances had become deposited in the middle lamella, periplasmic space, and vacuoles (Fig. 12K). Pectin accumulation was also evident in the cell walls and vacuoles of the haustorial protoderm (Fig. 12L).

Tests to identify lipid reserves (using neutral red) showed negative results in all structures during all of the evaluated phases of seeds with their operculum intact (initial condition, ligule expansion, and 180 days of cultivation).

Ultrastructural evaluations

In their initial condition, the cells of the embryo were organelle-poor, although there was evident storage of diverse metabolic

reserve substances. The protoderm cells of the cotyledonary petiole had thin walls, cytoplasm with abundant granular material (Fig. 13A–B), and a conspicuous nucleus with condensed chromatin (Fig. 13C); lipid droplets, small vesicles, and plastids were evident in the peripheral cytoplasm (Fig. 13B, D). The ground meristem cells had thin walls and a large central vacuole containing abundant granular material (Fig. 13E); smaller vacuoles and small lipid droplets surrounded the central vacuole and appeared along the periphery of the cytoplasm (Fig. 13F). Sinuities were evident in the plasma membrane, with accumulations of substances in the periplasmic spaces.

The cells of intact seeds, after 180 days of cultivation, showed increased internal activities, especially in the ground meristem, with organelles notably more differentiated and numerous as compared to the initial phase. The cytoplasm of the protoderm remained rich in granular substances and lipid droplets (Fig. 13G–H), with a proliferation of vesicles along the peripheries of the cells and their mitochondria, the latter being small and with poorly developed cristae (Fig. 13H–I). Plastids with well-differentiated internal membrane systems evidenced accumulated starch grains or lipophilic compounds (Fig. 13I–J); the plasma membrane was sinuous and there were accumulated substances in the periplasmic spaces (Fig. 13J). The cells of the ground meristem had vacuoles with only remnants of their reserve contents, indicating intense mobilization associated with the accumulation of phenolic compounds and vacuolation (Fig. 13K–L); there was a notable proliferation of vesicles along the periphery of the cytoplasm, with numerous amyloplasts, elaioplasts, and mitochondria around the nucleus (Fig. 13L).

Discussion

This is the first study focusing on germination and seedling development of the basal palm *M. armata*. Our results allowed us to identify associations between seed recalcitrance and dormancy, the role of cell divisions and expansions, and the dynamics of reserve compounds during the completion of germination, as well as to define its pattern of post-seminal development. This information contributes to the expansion of basic knowledge concerning palm tree reproduction and their evolutionary history, as *M. armata* is inserted within the subfamily Calamoideae, a sister group of the other lineages of Arecaceae (Baker and Couvreur 2013). This information can also subsidize the development of propagation technologies for this species, which is ecologically and socially important in the wetlands of South America.

Morphological aspects of germination completion and post-seminal development

The protrusion of the cotyledonary petiole signals the completion of germination of *M. armata* seeds (Fig. 1B). The

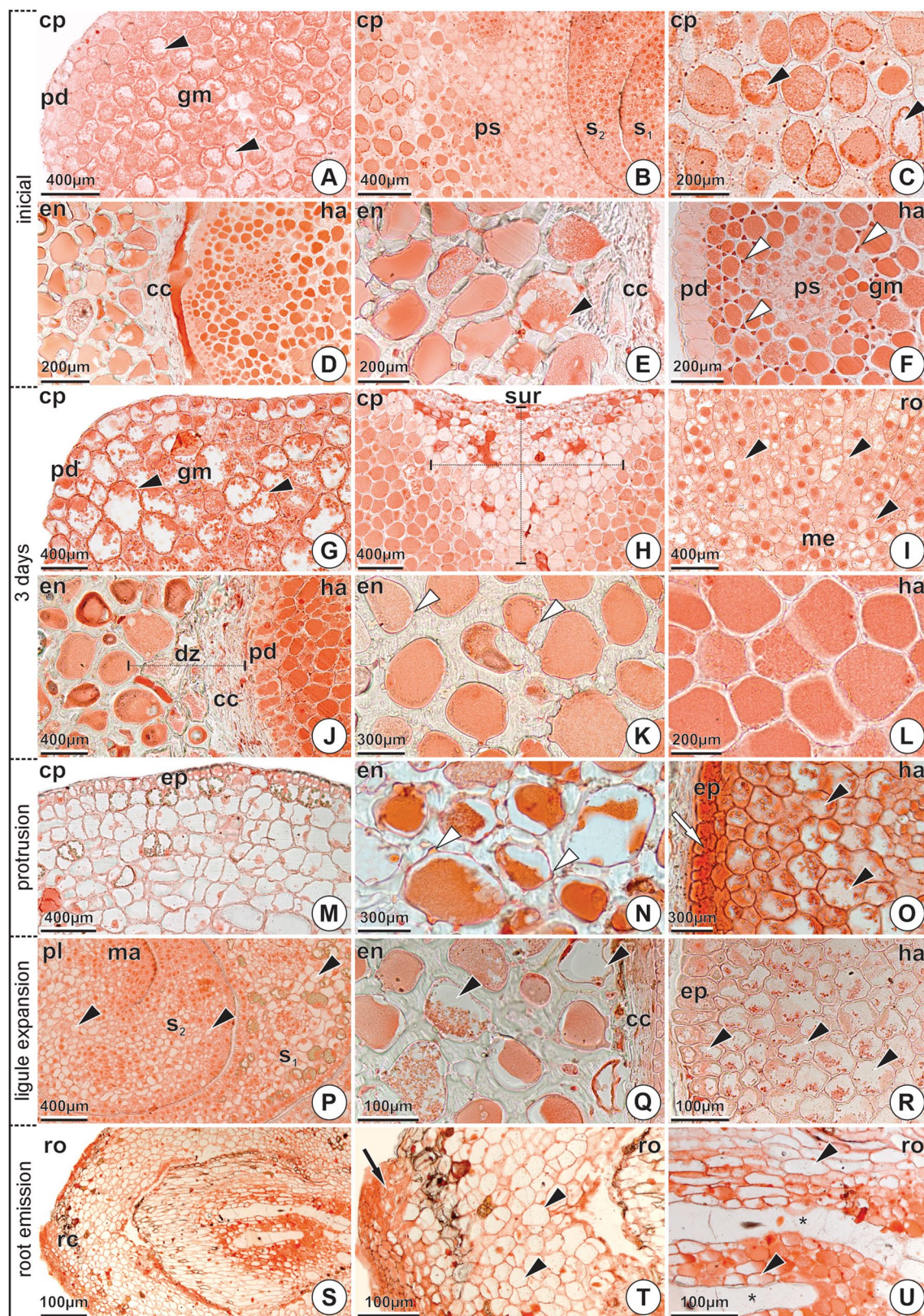


Fig. 9 Longitudinal (A–C, G–I, M, P, S–U) and cross (D–F, K–L, N–O, Q–R)-sections of seeds and seedlings of *Mauritiella armata* showing protein reserves stained red by the xyloidine-Ponceau (XP) test. The column on the left indicates the stage of development. Cotyledonary petiole with proteins stored in vacuoles and evidence of partial mobilization of reserves (black arrowheads) (A–C). Haustorium/endosperm interface showing abundant protein reserves, which are absent in the collapsed cell layer (D). Endosperm cells, highlighting partial consumption of reserves (arrowhead) and translocation by symplastic route through primary pit fields (E). Abundance of protein reserves in the haustorium, with extravasation into the intercellular space (white arrowhead) (F). Cotyledonary petiole with remnants of proteins on the periphery of the cells (arrowheads) (G). The suspensor region whose protein content was mostly mobilized (H). Region adjacent to the root apical meristem with accumulation of proteins (arrowheads) (I). Haustorium/endosperm interface showing expansion of the digestion zone (J). Endosperm cells showing mobilization of reserves in the periphery (arrowheads) and translocation by symplastic flow (K). Ground meristem cells of the haustorium with protein reserves (L). Proximal region of the cotyledonary petiole with absence of protein reserves in the parenchyma cells (M). Evidence of symplastic flow of proteins in the endosperm (arrowheads) (N). Haustorium with accumulation of proteins in the epidermis and adjacent layers (arrow) and granular material concentrated in the periphery of parenchyma cells (arrowheads) (O). Plumule, with partial mobilization of reserves (arrowheads) (P). Endosperm cells showing progress in reserve mobilization (arrowheads) (Q). Haustorium showing parenchyma cells with protein remnants (arrowheads) (R). Root with cells without protein reserves (arrowheads) (S–T), protein accumulation in the root cap (arrow) (T), and cells with partially mobilized reserves in the cortical region (arrowheads) (U). cc, layer of collapsed cells; cp, cotyledonary petiole; dz, digestion zone; en, endosperm; ep, epidermis; gm, ground meristem; ha, haustorium; ma, shoot apical meristem; me, root apical meristem; pd, protoderm; pl, plumule; ps, procambial strands; rc, root cap; ro, root; s1, first leaf sheath; s2, second leaf sheath; sur, suspensor region; (*), spaces formed by the fusion of raphidic idioblasts

species demonstrates a post-germination development pattern of the adjacent ligular type, characterized by the absence of accentuated growth of the cotyledonary petiole and involving the formation of a germinative bud from which the root and the aerial portion are emitted adjacent to the seed (Henderson 2006). This pattern is predominant in the Calamoideae and Arecoideae sub-families (Dransfield et al. 2008) and is considered a primitive feature among palms (Rocha 2022). Other palm species with the same pattern of development, such as *M. flexuosa* and *Euterpe precatoria* Mart., are also adapted to grow in swampy environments (Silva et al. 2014; Moura et al. 2019; Ferreira et al. 2020). This type of developmental pattern is considered to represent an adaptive advantage in these environments, as the initial development of the vegetative axis occurs close to the soil surface, with its more favorable access to oxygen (Moura et al. 2019).

Roles of cell division and expansion in the embryo/seedling transition

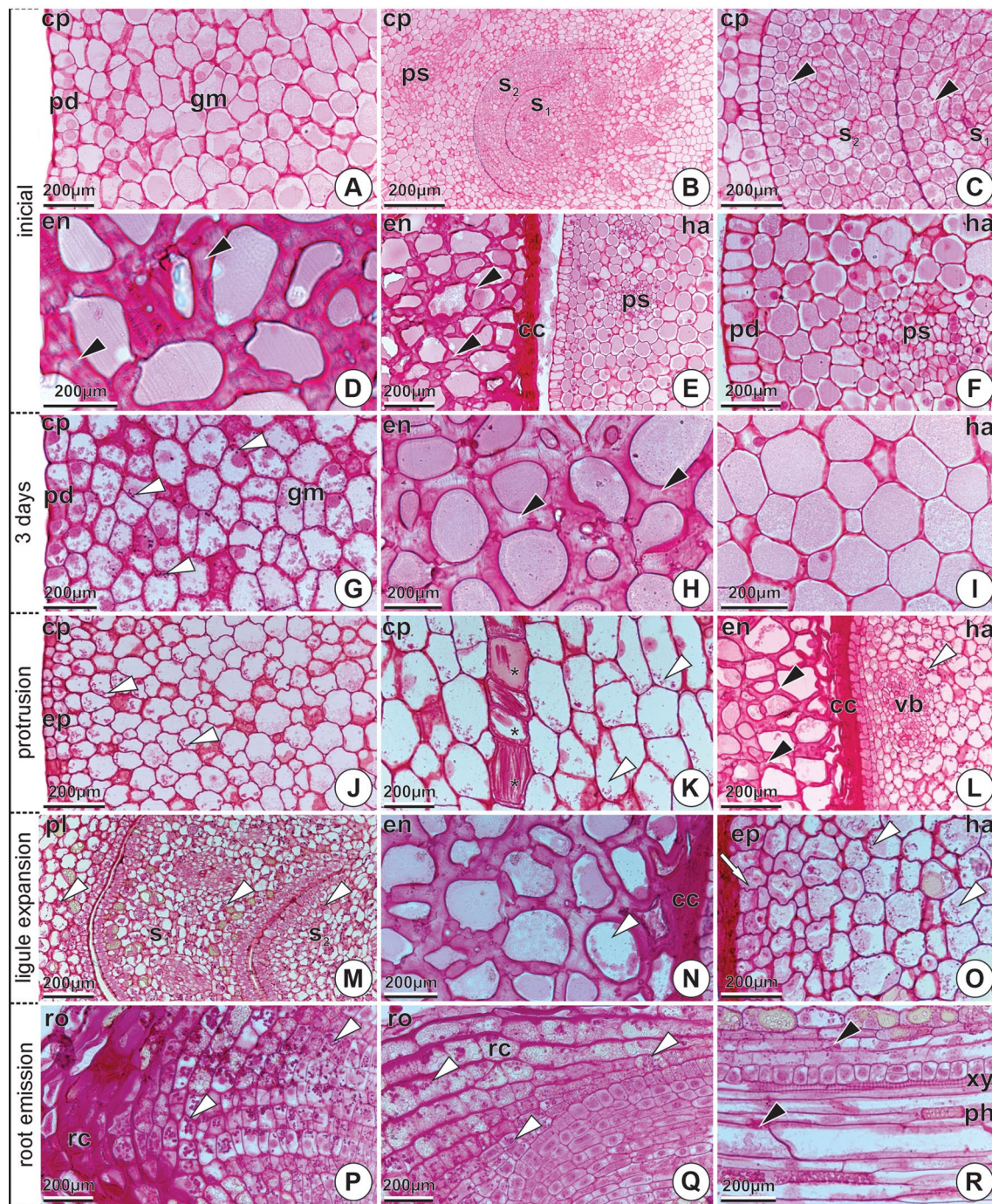
The germination and initial development of *M. armata* seeds reflect the association between cell divisions and cell

expansions in specific regions of the embryo/seedling. In most angiosperms, cell elongation (usually in the hypocotyl-radicle axis) is sufficient to promote the completion of germination (Bewley et al. 2013; Steinbrecher and Leubner-Metzger 2017). Palm seeds, however, have embryos with complex anatomies that do not follow this pattern (Mazzottini-dos-Santos et al. 2018). It was evident in the present study that the elongation of the cells of the hypocotyl-radicle axis, observed after 3 days of sowing (Fig. 14), represents one of the first indications of germination, as described in other palms (Ribeiro et al. 2012; Oliveira et al. 2013; Moura et al. 2019). This event is associated, however, with the occurrence of cell divisions in the periphery of the cotyledonary petiole and in procambial cords. The formation of the germinative bud, in turn, relies on the participation of meristematic regions in the proximal and median regions of the petiole, whose activities occur concomitantly with cell expansion related to the differentiation of the parenchyma (Fig. 14). The dependence on cell divisions in the cotyledonary petiole for the completion of palm germination has been related to the anatomy of the embryonic axis, which has only microscopic dimensions and therefore an only limited ability to overcome the resistance of the operculum (Oliveira et al. 2013; Moura et al. 2019). The influence of meristematic regions on germination and seedling development in palms was first proposed by DeMason (1984). The “M zone” (Haccius and Philip 1979) (the meristematic region between the protoderm and the root) contributes to the formation of the root cap as well as to the displacement of the operculum (Oliveira et al. 2013).

Cellular expansion occurs in a generalized manner 3 days after sowing in the different regions of the cotyledonary petiole of *M. armata*, although it is more expressive in the distal region (Fig. 14). This expansion process is associated with the differentiation of voluminous raphide idioblasts. The functions of those raphides (acicular crystals of calcium oxalate) are still being discussed (Paiva 2021), however, and it has been proposed that they are related to calcium storage (Zona 2004). During the development of *M. armata* seedlings, the raphidic idioblasts fuse—giving rise to large spaces in the cotyledonary petiole and root (Fig. 14). The expansion of haustorial parenchyma cells also results in the formation of an aerenchyma—which has been linked to the storage of the oxygen necessary to metabolize the endosperm reserves (DeMason 1984; Dias et al. 2020). Considering the adaptation of *M. armata* to swampy environments, these spaces in the haustorium and root may have similar functions related to oxygen storage.

Cellular composition and dynamics of reserve compounds during germination

The cellular composition of the embryo and endosperm of *M. armata* indicates the recalcitrant condition of the seeds.



Recalcitrance (intolerance to desiccation and low temperatures) is determined by the absence of quiescence (blockage of development due to desiccation in the pre-dispersal phase) and has crucial implications for seed behavior in soil banks and under storage conditions (Tweddle et al. 2003; Berjak and Pammenter 2008a, 2008b; Marques et al. 2018; Salvador et al. 2022). The identification of recalcitrance is commonly based on physiological studies of the behavior of stored seeds (Hong and Ellis 1996), although the integration of information related to cellular composition also allows

that diagnosis (Berjak and Pammenter 2000, 2008a, 2008b; Veloso et al. 2016).

The cytological characteristics associated with recalcitrance observed in the present work with *M. armata* seeds, and recognized in previous studies, include: (i) a water content greater than 40% in the seed and 80% in the embryo (Hong and Ellis 1996; Marques et al. 2018); (ii) reduced lipid reserves (Berjak and Pammenter 2000; Veloso et al. 2016); (iii) protein reserves associated with pectins and stored in large vacuoles (Veloso et al. 2016); (iv) restricted

Fig. 10 Longitudinal (A–C, G, J–K, M, P–R) and cross (D–F, H–I, L, N–O) sections of *Mauritiella armata* seeds and seedlings showing neutral polysaccharides revealed by magenta staining by periodic acid and Schiff-PAS reagent. The column on the left indicates the stage of development. Cotyledonary petiole (A) and plumule (B) with neutral polysaccharides in the vacuoles. Indicative of partial mobilization of reserves in the plumule (arrowheads) (C). Endosperm cells with accumulation of reserves in the vacuole and, mainly, in the cell walls; areas of the cell wall with evidence of partial mobilization (arrowheads) (D). Haustorium/endosperm interface with accumulation of polysaccharides in endosperm cells, collapsed cell layers, and in haustorium cells; endosperm cells show some areas with partial mobilization (arrowheads) (E). Detail of the accumulation of neutral polysaccharides in vacuoles and cell walls at the periphery of the haustorium (F). Cotyledonary petiole showing starch grain and remnants of flocculated material (arrowheads) (G). Endosperm cells with areas of mobilization in cell walls (arrowheads) (H). Haustorium cells showing maintenance of neutral polysaccharides reserves (I). Periphery of the cotyledonary petiole with cells showing the remnants of reserves with a flocculated appearance (arrowheads) (J). Internal region of the cotyledonary petiole with cells in an advanced phase of mobilization of reserves, with remnants with a flocculated aspect (K). Haustorium/endosperm interface showing deposition of reserves in the endosperm cell walls (arrowheads) and starch grains in the haustorium (white arrowhead) (L). Plumule region with starch grains (arrowheads) (M). Endosperm cells, showing evidence of reserve mobilization in vacuoles (arrowhead) (N). Periphery of the haustorium with accumulation of neutral polysaccharides in the cell walls of the epidermis (arrow) and starch grains in the parenchyma cells (arrowheads) (O). Accumulation of neutral polysaccharides and starch grains (arrowheads) in the root cap (P–Q). Deposition of neutral polysaccharides in the vascular cylinder of the root (R). cc, collapsed cell layers; cp, cotyledonary petiole; en, endosperm; ep, epidermis; gm, ground meristem; ha, haustorium; pd, protoderm; ph, phloem; pl, plumule; ps, procambial strands; rc, root cap; ro, root; s1, first leaf sheath; s2, second leaf sheath; vb, vascular bundle; xy, xylem; (*), raphidic idioblasts

cytoplasm (Panza et al. 2004; Dias et al. 2020); and (v) significant accumulations of phenolic compounds during seedling development (Moura et al. 2019). Additionally, there is evidence of the mobilization of proteins (Fig. 9A–C, E) and neutral polysaccharides (Fig. 10B–C) in the embryo and endosperm, and a flux of pectic substances in the endosperm (Fig. 11B) in newly dispersed seeds, which suggests their occurrence in the pre-dispersal phase. These processes, combined with the presence of differentiated vessel elements in the embryo (also observed in *M. flexuosa*; Silva et al. 2014), can be associated with the continuous development related to recalcitrance (Veloso et al. 2016). Recalcitrance favors the adaptation to flooded environments, but also commonly restricts those species' distributions to humid habitats (Tweddle et al. 2003; Marques et al. 2018). Thus, it is likely that this condition is an important component of that niche and conditions the spatial distribution of *M. armata*.

The dynamics of reserve compound during the germination and early development of *M. armata* involve embryo/seedling and endosperm interactions, mobilization, and deposition of those compounds in specific regions, and their translocation through symplastic and apoplastic

pathways. Reserve mobilization in the cotyledonary petiole and endosperm in *M. armata* is precocious as compared to other palm species (Oliveira et al. 2013; Mazzottini-dos-Santos et al. 2017), including species that evidence recalcitrant behaviors (Panza et al. 2004; Moura et al. 2019; Dias et al. 2020; Ferreira et al. 2020). The mobilization of neutral polysaccharides results in the formation of transient starch grains 3 days after sowing, with the intensification of their deposition in growth regions in later stages and the simultaneous reduction of mucilaginous reserves (Fig. 14). These results are in line with other studies that attest to the importance of starch reserves during the growth of palm seedlings (Mazzottini-dos-Santos et al. 2017; Dias et al. 2018).

Throughout the mobilization of protein and pectic reserves, those compounds become concentrated in the protodermis/epidermis of the haustorium (Fig. 9O, 11k–L) and cotyledonary petiole (Fig. 14), concomitant with their reduction in the endosperm (Fig. 9K, N, Q, 11H). The roles of these structures in the dynamics of reserve mobilization in palm seeds have been described in other studies (DeMason 1985; Mazzottini-dos-Santos et al. 2017; Dias et al. 2018; Moura et al. 2019; Dias et al. 2020). The haustorium mobilizes its own reserves, and acts in the absorption and translocation of reserves from the endosperm to the cotyledonary petiole, from which they are subsequently directed to the vegetative axis (DeMason 1981; Moura et al. 2019; Dias et al. 2020). The haustorium also induces the mobilization of endosperm reserves through oxygen diffusion, and increases the contact surface and pressure on this tissue due to its growth (Mazzottini-dos-Santos et al. 2017; Dias et al. 2018). Our results indicate that the haustorium protoderm cell wall villi and projections favor the increased absorption capacity of endospermic reserves in *M. armata* (Fig. 2A, D).

The integration of the symplastic and apoplastic pathways observed in the embryo/seedling and endosperm of *M. armata* contributes to the efficiency of reserve mobilization. The flow of endosperm reserves initially occurs through symplastic flow through the primary pit fields (Fig. 9N, 11B), and is followed by apoplastic flow (Fig. 10L)—a pattern similar to that described for the palm *M. flexuosa* (Dias et al. 2020). Apoplastic flow predominates through cell walls and intercellular spaces in the embryo/seedling (Fig. 9F, 11 G, I, J–L). The combination of these two translocation pathways is one possible explanation for the faster mobilization of reserves in *M. armata* seeds in relation to the other palms (Dias et al. 2020; Mazzottini-dos-Santos et al. 2020). There is an intense accumulation of hydrophilic pectic substances during the initial development of *M. armata* (Fig. 14), and they may contribute to the maintenance of the hydrated water status essential to seedling homeostasis. These aspects likely contribute to the establishment of seedlings in the midst of dense herbaceous vegetation and in environments with seasonal climates, such as the “veredas” of the Cerrado biome.

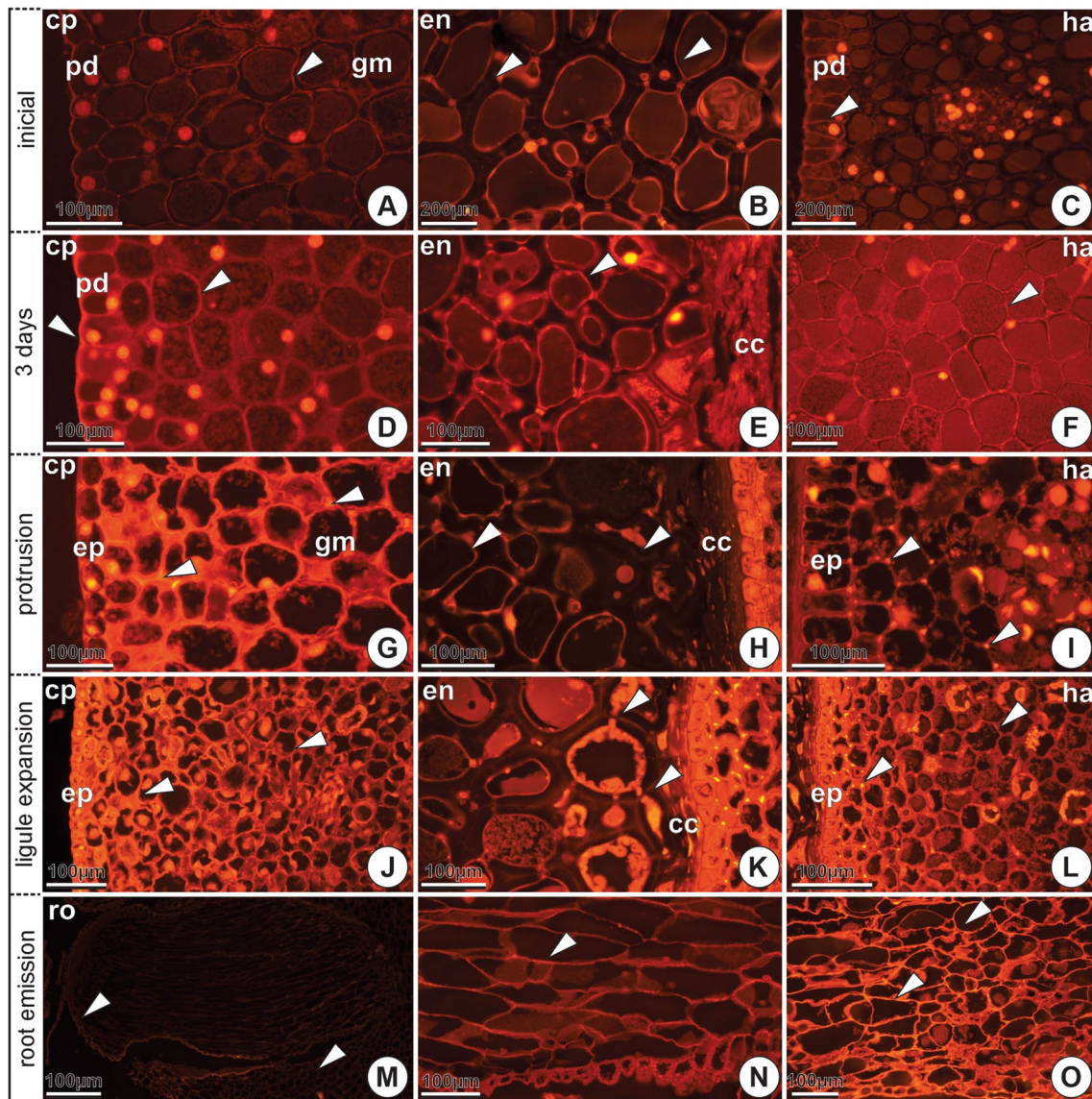


Fig. 11 Longitudinal (A, D, G, J, M–O) and cross (B–C, E–F, H–I, K–L)-sections of seeds and seedlings of *Mauritiella armata* showing acidic polysaccharides (pectins) highlighted by orange fluorescence by choriphosphine. The column on the left indicates the stage of development. Pectins (arrowheads) in the middle lamella and cell walls of the cotyledonary petiole (A), inner cell walls, median lamella and endosperm vacuoles (B), and cell walls of the haustorium protoderm (C). Accumulation of pectins (arrowheads) in the outer cell walls of the protoderm, cell walls, vacuoles, and middle lamella of the ground meristem of the cotyledonary petiole (D). Accumulation of pectins (arrowhead) in the middle lamella, internal walls, and vacuoles of the endosperm (E). Accumulation of pectins in vacuoles and cell walls (arrowhead) in the haustorium parenchyma (F). Cotyledon-

ary petiole showing abundance of pectic substances, with emphasis on the intercellular spaces (arrowheads) (G). Evidence of mobilization of pectic substances in the endosperm, with concentration in the periplasmic space (arrowheads) (H). Haustorium with evidence of mobilization and extravasation of pectins in the intercellular spaces (arrowheads) (I). Accumulation of pectins (arrowheads) in the epidermis and parenchyma of the cotyledonary petiole (J). Evidence of symplastic flow of pectic substances into the endosperm (arrowheads) (K). Accumulation of pectins (arrowheads) in the epidermis and parenchyma of the haustorium (L). Root, showing accumulation of pectins in cell walls (M–O). cc, layer of collapsed cells; cp, cotyledonary petiole; en, endosperm; ep, epidermis; gm, ground meristem; ha, haustorium; pd, protoderm; ro, root

Changes in dormant seeds over time

M. armata seeds exhibit dormancy. Seeds with their opercula mechanically removed germinate within a few days, while intact seeds, sown under the same conditions, do not

germinate for 180 days. Baskin and Baskin (2014a) consider that the absence of germination for 30 days under favorable conditions characterizes dormancy. As with other angiosperm seeds, palm germination is controlled by the ability of the embryo to overcome the resistance imposed by

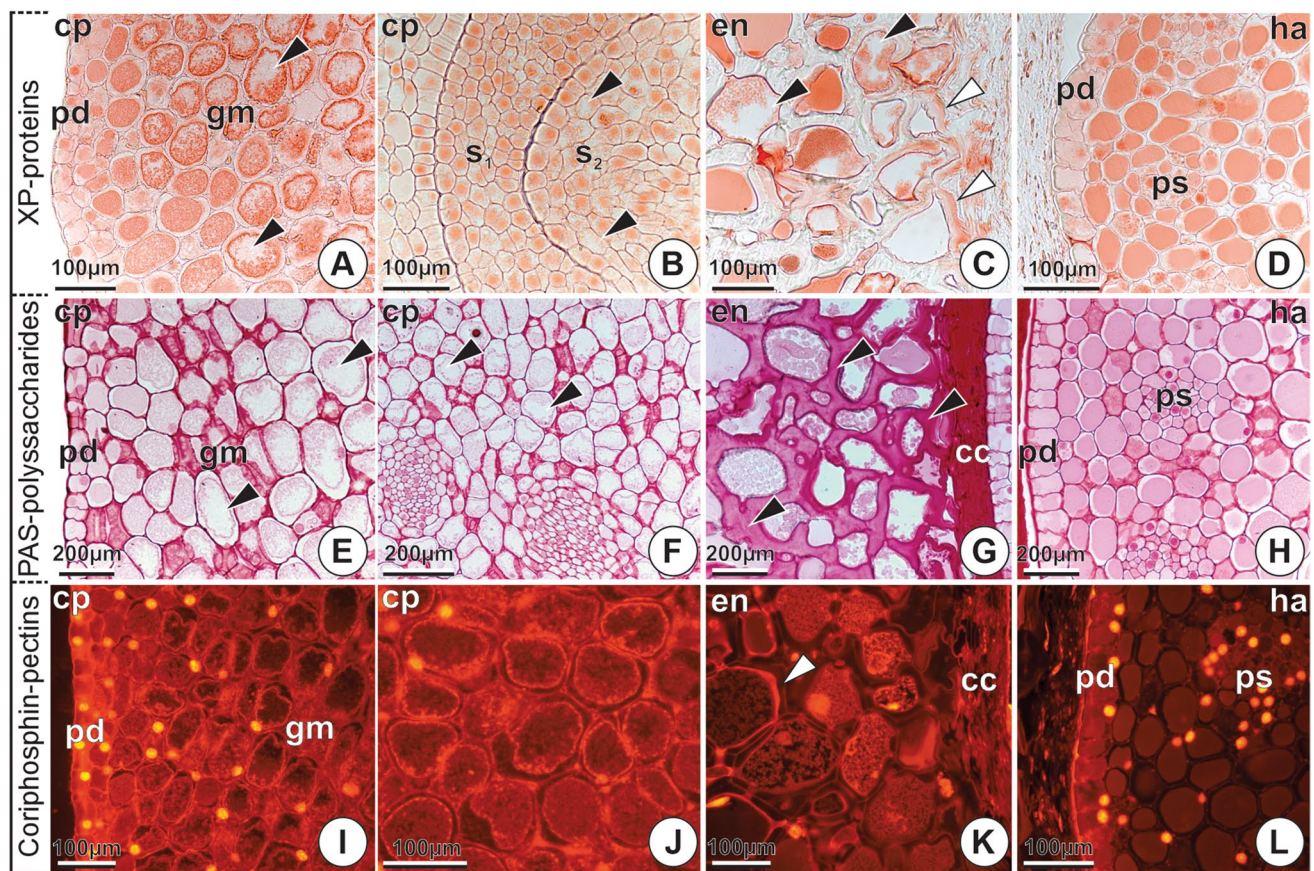


Fig. 12 Longitudinal (A–B, E–F, I–J) and cross (C–D, G–H, K–L) sections of dormant *Mauritiella armata* seeds, after 180 days of sowing, submitted to histochemical tests. The dyes and identified substances are listed in the left column. Cotyledonary petiole (A) and plumule region (B), showing partial mobilization of protein reserves (arrowheads). Areas with partial mobilization of protein reserves in endosperm cells (black arrowheads) and evidence of translocation, by symplastic flow, and accumulation in the collapsed cell layers (white arrowheads) (C). Haustorium with abundant protein reserves in the vacuoles of ground meristem cells (D). Cotyledonary petiole showing remnants of neutral polysaccharides with a flocculated appearance in the ground meristem cells (arrowheads) (E–F). Indicative

of the mobilization of reserves in the vacuoles and emphasis on the accumulation of substances in the cell walls (arrowheads) of the endosperm adjacent to the haustorium (G). Haustorium with abundance of neutral polysaccharides in the vacuoles (H). Pectins found in abundance in the vacuoles, cell walls, and middle lamella in the protoderm and ground meristem of the cotyledonary petiole (I–J), protoderm of the haustorium (L), and vacuoles and periplasmic spaces of the endosperm (arrowhead) (K). cc, layer of collapsed cells; cp, cotyledonary petiole; en, endosperm; gm, ground meristem; ha, haustorium; pd, protoderm; ps, procambial strand; s1, first leaf sheath; s2, second leaf sheath

adjacent tissues (Steinbrecher and Leubner-Metzger 2017; Mazzottini-dos-Santos et al. 2018). The operculum of palm seeds, formed by the opercular tegument and micropylar endosperm, offers the embryo protection but also limits its growth, thus contributing to the maintenance of dormancy (Ribeiro et al. 2011; Silva et al. 2014; Mazzottini-dos-Santos et al. 2018).

Dormancy has great ecological importance because it distributes germination over time and allows for the formation of seed banks (Finch-Savage and Leubner-Metzger 2006; Baskin and Baskin 2014b). The association between dormancy and recalcitrance is a rare condition, and has been reported in only 9% of species in a large study (Tweddle et al. 2003). Recent work has shown that, although

recalcitrant, dormant *M. flexuosa* seeds form persistent seed banks in humid environments (Salvador et al. 2022). *M. armata* and *M. flexuosa* (both Calamoideae, Mauritiaceae, Dransfield et al. 2008) share many characteristics, among them the abundance of mucilage in their seeds and an association between dormancy and recalcitrance.

The dormant seeds of *M. armata* show remarkable changes over time that are related to tissue differentiation and the mobilization of embryonic and endospermic reserves indicative of high cellular activity levels. During the incubation of dormant *M. armata* seeds, protein reserve mobilization intensifies in the cotyledonary petiole and endosperm (Fig. 12A–C) and the neutral polysaccharides of the cotyledonary petiole are largely mobilized

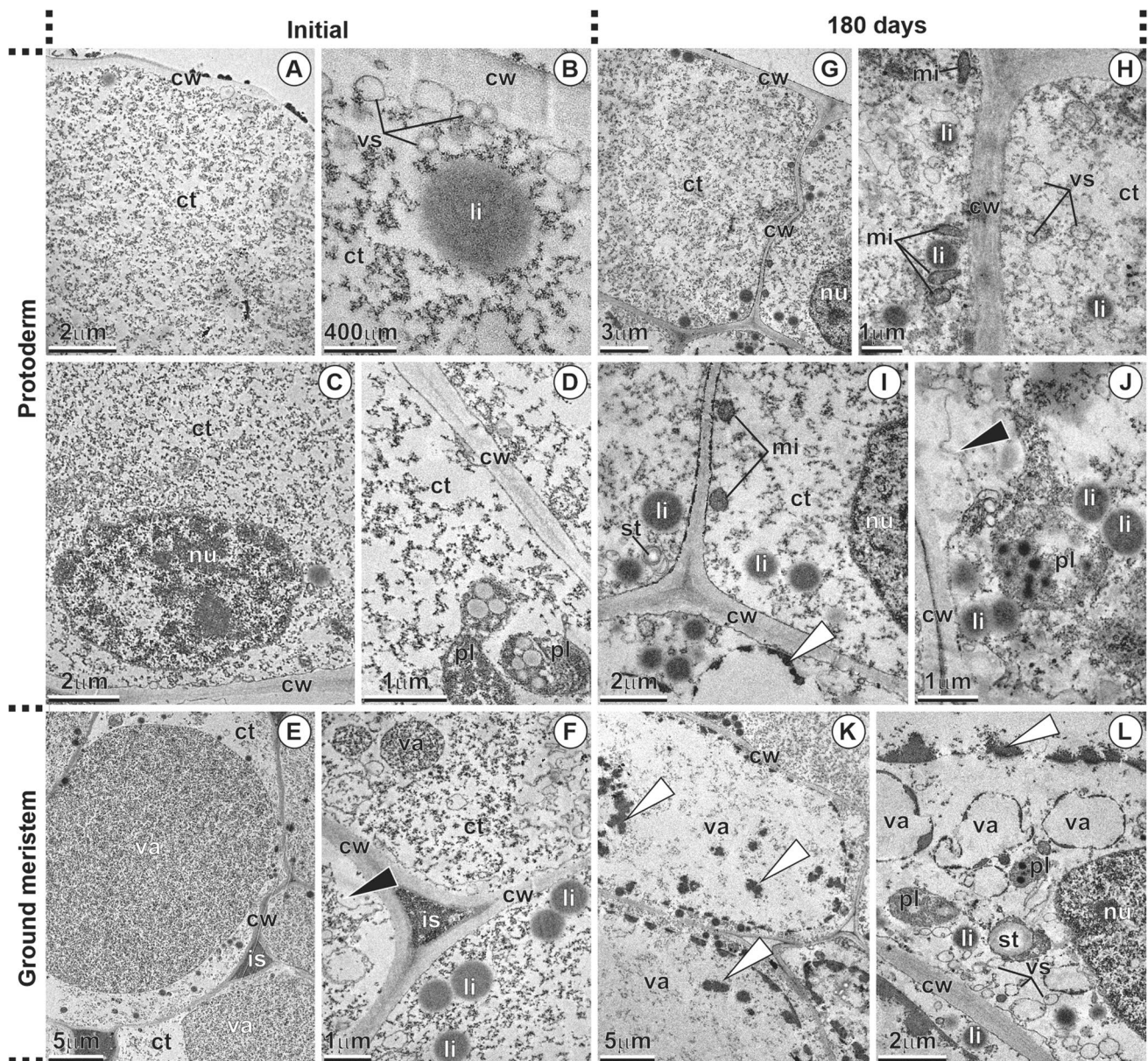


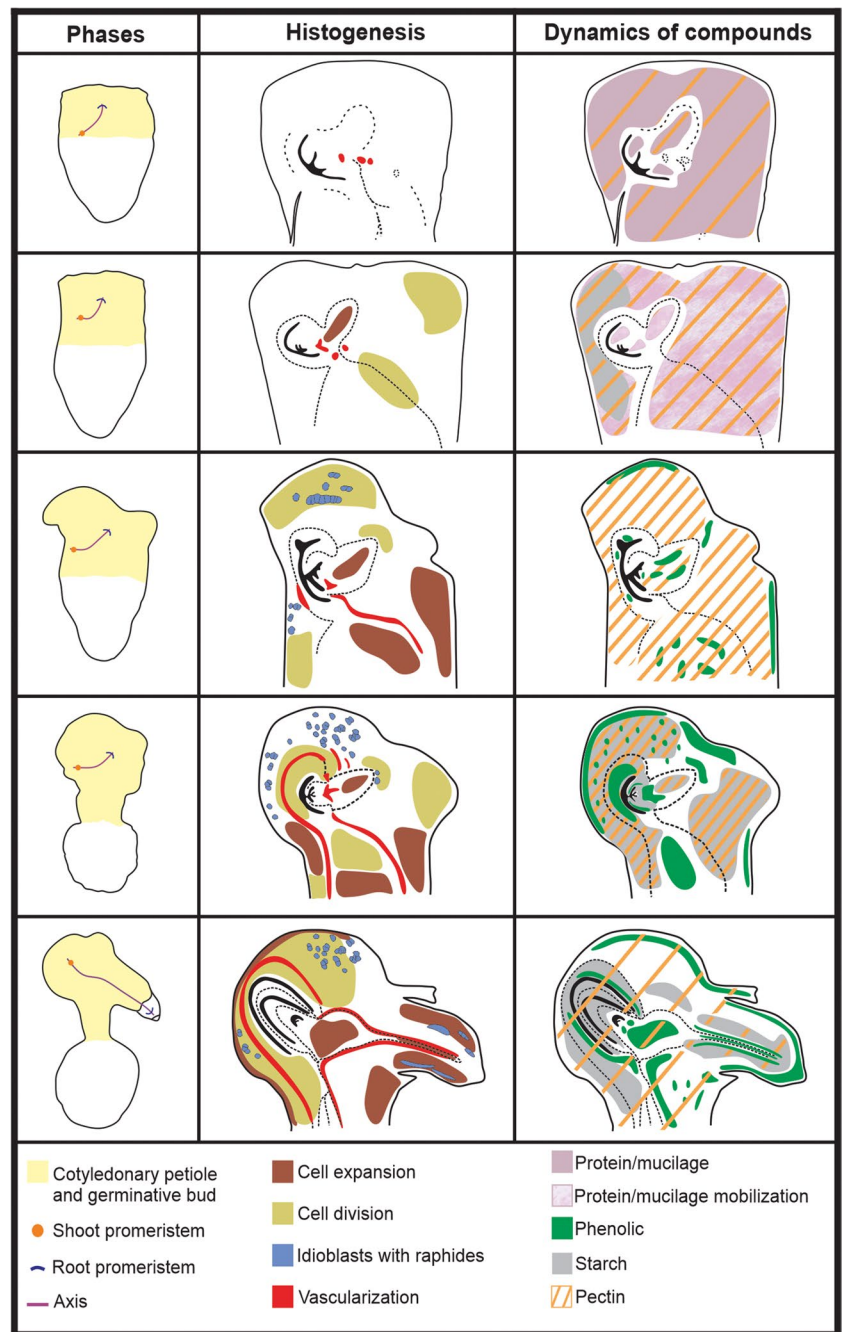
Fig. 13 Images obtained by transmission electron microscopy of the protoderm and ground meristem of the cotyledonary petiole of *Mauritiella armata* embryos. Newly dispersed seeds (A–F) and dormant seeds, 180 days after sowing (G–L). Cytoplasm containing granular material (A); cell periphery with vesicles and lipid droplets (B); conspicuous nucleus (C) and plastids (D). Voluminous vacuole containing granular material (E); sinuosity of the plasma membrane (arrow-

head) (F). Proliferation of mitochondria, vesicles, and lipid droplets at the periphery of the cell (G–H). Plastid proliferation and plasma membrane sinuosity (black arrowhead) (I–J). Reserve remnants in the vacuole and accumulation of phenolic compounds (arrowheads) (K–L); vacuolation and proliferation of vesicles (L). ct, cytosol; cw, cell wall; is, intercellular space; li, lipid; mi, mitochondria; nu, nucleus; pl, plastid; st, starch; va, vacuole; vs, vesicles

(Fig. 12E–F). Mobilization of the vacuolar contents of the endosperm and their deposition in the cell walls are likewise evident (Fig. 12G), with accumulations of pectins in the cotyledonary petiole and protoderm of the haustorium and the flow of reserve substances in the endosperm (Fig. 12I–L). Vacuolation also occurs in embryonic cells (Fig. 13L), together with the accumulation of starch grains

and phenolic compounds and the proliferation of vesicles and mitochondria (Fig. 13H) that indicate increased cellular activity. These processes are similar to those described in the dormant seeds of *M. flexuosa* (Moura et al. 2019), and are associated with the continuous development inherent to recalcitrance, and, on the other hand, to the gradual overcoming of dormancy. These results, taken together,

Fig. 14 Scheme showing morphogenesis and compound dynamics during germination and early seedling development of *Mauritiella armata*. The column on the left indicates the stages of development



suggest that *M. armata* seeds, despite their recalcitrant condition, have the capacity to maintain soil seed banks in which seeds develop only slowly until dormancy is overcome.

Conclusions

The results obtained in the present work allow us to conclude that *M. armata* seeds demonstrate both recalcitrance and dormancy. The cytological characteristics of the embryo and

endosperm of *M. armata* indicate a recalcitrant condition of the seeds. The germination and the initial development of its seedlings are characterized by associations between cell divisions and expansions occurring in specific regions. The mobilization of seminal reserves involves embryo/seedling and endosperm interactions and their translocation through both the symplastic and apoplastic pathways. Dormant intact seeds, after 180 days of cultivation, show cell divisions in the embryo, mobilization of embryonic and endospermic reserves, and indications of high cellular activity, which all contribute to overcoming dormancy. The anatomical and

histochemical characteristics of *M. armata* seeds, as well as their germination pattern, contribute to the successful adaptation of this species to humid environments and its reproductive success.

Acknowledgements The authors thank Dr. Sarah Barbosa Reis for reviewing the text and the Centro de Microscopia da Universidade Federal de Minas Gerais - CM/UFMG for making its infrastructure available for the electron microscopy analyses.

Author contribution LMR, HCM-S, IFPA, and YRFN idealized and planned the research. PPF collected and processed the plant material, prepared anatomical slides and electronic microscopy samples, and wrote the initial text. LMR and PPF performed the anatomical analyses. HCM-S analyzed histochemical and electron microscopy data. LMR, PPF, and HCM-S elaborated the final text. All authors have read and approved the manuscript.

Funding This research was supported by the Long Term Ecological Research Network (Programa de Pesquisa Ecológica de Longa Duração – PELD-VERE) of the National Council for Scientific and Technological Development – CNPq (Edital 093/2021); the Fundação de Amparo à Pesquisa do Estado de Minas Gerais – FAPEMIG (APQ-03371-21); and the Ministry of Science, Technology and Innovations – MCTI, Brazil. The authors are grateful to FAPEMIG and CNPq for the master's scholarship granted to PPF, and to CNPq for the research productivity scholarships granted to LMR and YRFN.

Declarations

Conflict of interest The authors declare no competing interests.

References

- Ávila MA, Azevedo IFP, Antunes JR, Souza CR, Santos RM, Fonseca RS, Nunes YRF (2022) Temperature as the main factor affecting the reproductive phenology of the dioecious palm *Mauritiella armata* (Arecaceae). *Acta Botan Brasil* 36:1–12. <https://doi.org/10.1590/0102-33062021abb0111>
- Ávila MAD, Nunes YRF, Souza CS, Machado ADO, Mazzottini-dos-Santos HC, Ribeiro LM, Santos RMD, De Azevedo IFP (2023) Local environment contributes to shape phenological patterns in *Mauritia flexuosa* L.f. *For Ecol Manage* 545:121252. <https://doi.org/10.1016/j.foreco.2023.121252>
- Baker WJ, Couvreur TLP (2013) Global biogeography and diversification of palms sheds light on the evolution of tropical lineages. I. Historical biogeography. *J Biogeogr* 40:274–285. <https://doi.org/10.1111/j.1365-2699.2012.02795.x>
- Baskin CC, Baskin JM (2014) Seeds: ecology, biogeography, and evolution of dormancy and germination. Elsevier/AP, San Diego
- Baskin JM, Baskin CC (2014) What kind of seed dormancy might palms have? *Seed Sci Res* 24:17–22. <https://doi.org/10.1017/S0960258513000342>
- Baskin JM, Baskin CC (2021) The great diversity in kinds of seed dormancy: a revision of the Nikolaeva-Baskin classification system for primary seed dormancy. *Seed Sci Res* 31:249–277. <https://doi.org/10.1017/S096025852100026X>
- Berjak P, Pammenter NW (2000) What ultrastructure has told us about recalcitrant seeds. *Rev Bras Fisiol Veg* 12:22–55
- Berjak P, Pammenter NW (2008) From Avicennia to Zizania: seed recalcitrance in perspective. *Ann Bot* 101:213–228
- Berjak P, Pammenter NW (2008) Perspectives on seed recalcitrance. *S Afr J Bot* 74:361. <https://doi.org/10.1016/j.sajb.2008.01.032>
- Bewley JD, Bradford KJ, Hilhorst HWM, Nonogaki H (2013) Seeds: physiology of development, germination and dormancy, 3rd edn. Springer, New York
- Brasil (Ministério da Agricultura Pecuária e Abastecimento) (2009) Regras para análise de sementes. Mapa/ACS, Brasília, DF
- Carvalho VS, Ribeiro LM, Lopes PSN et al (2015) Dormancy is modulated by seed structures in palms of the cerrado biome. *Aust J Bot* 63:444. <https://doi.org/10.1071/BT14224>
- da Neves SC, Ribeiro LM, da Cunha IRG et al (2013) Diaspore structure and germination ecophysiology of the babassu palm (*Attalea vitrivir*). *Flora* 208:68–78. <https://doi.org/10.1016/j.flora.2012.12.007>
- DeMason DA (1984) Growth parameters in the cotyledon of date seedlings. *Bot Gaz* 145:176–183. <https://doi.org/10.1086/337444>
- DeMason DA, Thomson WW (1981) Structure and ultrastructure of the cotyledon of date palm (*Phoenix dactylifera* L.). *Bot Gaz* 142:320–328. <https://doi.org/10.1086/337230>
- DeMason DA, Sexton R, Gorman M, Reid JSG (1985) Structure and biochemistry of endosperm breakdown in date palm (*Phoenix dactylifera* L.) seeds. *Protoplasma* 126:159–167. <https://doi.org/10.1007/BF01281791>
- Dias DS, Ribeiro LM, Lopes PSN et al (2018) Haustorium–endosperm relationships and the integration between developmental pathways during reserve mobilization in *Butia capitata* (Arecaceae) seeds. *Ann Bot* 122:267–277. <https://doi.org/10.1093/aob/mcy065>
- Dias GP, Mazzottini-dos-Santos HC, Ribeiro LM et al (2020) Reserve mobilization dynamics and degradation pattern of mannan-rich cell walls in the recalcitrant seed of *Mauritia flexuosa* (Arecaceae). *Plant Physiol Biochem* 156:445–460. <https://doi.org/10.1016/j.plaphy.2020.09.03>
- Donohue K, Rubio de Casas R, Burghardt L, Kovach K, Willis CG (2010) Germination, postgermination adaptation, and species ecological ranges. *Annu Rev Ecol Evol Syst* 41:293–319. <https://doi.org/10.1146/annurev-ecolsys-102209-144715>
- Dransfield J, Uhl NW, Asmussen CBA, Baker WJ, Harley MM, Lewis CE (2008) *Genera Palmarum: the evolution and classification of palms*. New. Kew Publ, Royal Botanical Garden, Kew
- Feder N, O'Brien TP (1968) Plant microtechnique: some principles and new methods. *Am J Bot* 55:123. <https://doi.org/10.2307/2440500>
- Ferreira CD, de Silva-Cardoso IMA, Ferreira JCB et al (2020) Morphostructural and histochemical dynamics of *Euterpe precatoria* (Arecaceae) germination. *J Plant Res* 133:693–713. <https://doi.org/10.1007/s10265-020-01219-7>
- Finch-Savage WE, Leubner-Metzger G (2006) Seed dormancy and the control of germination: Tansley review. *New Phytol* 171:501–523. <https://doi.org/10.1111/j.1469-8137.2006.01787.x>
- Haccius B, Philip VJ (1979) Embryo development in *Cocos nucifera* L.: a critical contribution to a general understanding of palm embryogenesis. *Plant Syst Evol* 132:91–106. <https://doi.org/10.1007/BF00983086>
- Henderson FM (2006) Morphology and anatomy of palm seedlings. *Bot. Rev.* 72:273–329
- Hong TD, Ellis RH (1996) A protocol to determine seed storage behaviour. In: Engels JMM, Toll J (eds) IPGRI Technical Bulletin No. 1. International Plant Genetic Resources Institute, Rome
- Karnovsky MJA (1965) A formaldehyde-glutaraldehyde fixate of high osmolality for use in electron microscopy. *J Cell Biol* 27:137A–138A
- Kirk PW (1970) Neutral red as a lipid fluorochrome. *Stain Technol* 45:1–4. <https://doi.org/10.3109/10520297009063373>
- Lorenzi H, Noblick LR, Kahn F, Ferreira E (2010) *Flora Brasileira – Arecaceae (palmeiras)*. Instituto Plantarum, Nova Odessa

- Marques A, Buijs G, Ligterink W, Hilhorst H (2018) Evolutionary ecophysiology of seed desiccation sensitivity. *Funct Plant Biol* 45:1083. <https://doi.org/10.1071/FP18022>
- Mazzottini-dos-Santos HC, Ribeiro LM, Oliveira DMT (2017) Roles of the haustorium and endosperm during the development of seedlings of *Acrocomia aculeata* (Arecaceae): dynamics of reserve mobilization and accumulation. *Protoplasma* 254:1563–1578. <https://doi.org/10.1007/s00709-016-1048-x>
- Mazzottini-dos-Santos HC, Ribeiro LM, Oliveira DMT (2018) Structural changes in the micropylar region and overcoming dormancy in Cerrado palms seeds. *Trees* 32:1415–1428. <https://doi.org/10.1007/s00468-018-1723-y>
- Mazzottini-dos-Santos HC, Ribeiro LM, Oliveira DMT, Paiva EAS (2020) Ultrastructural aspects of metabolic pathways and translocation routes during mobilization of seed reserves in *Acrocomia aculeata* (Arecaceae). *Braz J Bot* 43:589–600. <https://doi.org/10.1007/s40415-020-00622-7>
- Moura ACF, Ribeiro LM, Mazzottini-dos-Santos HC et al (2019) Cytological and histochemical evaluations reveal roles of the cotyledonary petiole in the germination and seedling development of *Mauritia flexuosa* (Arecaceae). *Protoplasma* 256:1299–1316. <https://doi.org/10.1007/s00709-019-01375-1>
- Nunes YRF, Souza CS, Azevedo IFPD et al (2022) Vegetation structure and edaphic factors in veredas reflect different conservation status in these threatened areas. *For Ecosyst* 9:100036. <https://doi.org/10.1016/j.fecs.2022.100036>
- O'Brien TP, Feder N, McCully ME (1964) Polychromatic staining of plant cell walls by toluidine blue O. *Protoplasma* 59:368–373
- Oliveira NCC, Lopes PSN, Ribeiro LM et al (2013) Seed structure, germination, and reserve mobilization in *Butia capitata* (Arecaceae). *Trees* 27:1633–1645. <https://doi.org/10.1007/s00468-013-0910-0>
- Orozco-Segovia A, Batis AI, Rojas-Aréchiga M, Mendonza A (2003) Seed biology of palms: a review. *Palms* 47:79–74
- Paiva EAS (2021) Do calcium oxalate crystals protect against herbivory? *Sci Nat* 108:24. <https://doi.org/10.1007/s00114-021-01735-z>
- Paiva EAS, Pinho SZ, Oliveira DMT (2011) Large plant samples: how to process for GMA embedding? In: Melo RCN (ed) Choarini-Garcia H. *Methods and Protocols*. Humana Press Totowa, Light Microscopy, pp 37–49
- Panza V, Láinez V, Maldonado S (2004) Seed structure and histochemistry in the palm *Euterpe edulis*. *Bot J Linn Soc* 145:445–453. <https://doi.org/10.1111/j.1095-8339.2004.00293.x>
- Reis SB, Mello ACMP, Oliveira DMT (2017) Pericarp formation in early divergent species of Arecaceae (Calamoideae, Mauritiaceae) and its ecological and phylogenetic importance. *Plant Syst Evol* 303:675–687. <https://doi.org/10.1007/s00606-017-1399-6>
- Reynolds ES (1963) The use of lead citrate at high pH as an electron-opaque stain in electron microscopy. *J Cell Biol* 17:208–212. <https://doi.org/10.1083/jcb.17.1.208>
- Ribeiro LM, Souza PP, Rodrigues AG Jr et al (2011) Overcoming dormancy in macaw palm diaspores, a tropical species with potential for use as bio-fuel. *Seed Sci Technol* 39:303–317. <https://doi.org/10.15258/sst.2011.39.2.04>
- Ribeiro LM, Oliveira DMT, de Garcia Q, S, (2012) Structural evaluations of zygotic embryos and seedlings of the macaw palm (*Acrocomia aculeata*, Arecaceae) during in vitro germination. *Trees* 26:851–863. <https://doi.org/10.1007/s00468-011-0659-2>
- Ribeiro LM, Garcia QS, Müller M, Munné-Bosch S (2015) Tissue-specific hormonal profiling during dormancy release in macaw palm seeds. *Physiol Plantarum* 153:627–642. <https://doi.org/10.1111/ppl.12269>
- Robards AW (1978) An introduction to techniques for scanning electron microscopy of plant cells. In: Hall JL (ed) *Electron microscopy and cytochemistry of plant cells*. Elsevier, New York, pp 343–403
- Rocha, (2022) Crescimento geotrópico positivo do pecíolo cotiledonar em *Butia capitata* e implicações ecológicas e filogenéticas em palmeiras. Universidade Estadual de Montes Claros, Dissertação
- Roland AM (1978) General preparations and staining of thin sections. In: Hall JL (ed) *Electron microscopy and cytochemistry of plant cells*. Elsevier, New York, pp 1–62
- Salvador HF, Mazzottini-dos-Santos HC, Dias DS et al (2022) The dynamics of *Mauritia flexuosa* (Arecaceae) recalcitrant seed banks reveal control of their persistence in marsh environments. *For Ecol Manage* 511:120155. <https://doi.org/10.1016/j.foreco.2022.120155>
- Silva RS, Ribeiro LM, Mercadante-Simões MO et al (2014) Seed structure and germination in buriti (*Mauritia flexuosa*), the Swamp palm. *Flora* 209:674–685. <https://doi.org/10.1016/j.flora.2014.08.012>
- Smith N (2015) *Mauritiella armata*. Palms and people in the Amazon. Springer International Publishing, Cham, pp 383–389
- Souza JN, Ribeiro LM, Mercadante-Simões MO (2016) Ontogenesis and functions of saxophone stem in *Acrocomia aculeata* (Arecaceae). *Ann Bot* 119:353–365. <https://doi.org/10.1093/aob/mcw215>
- Souza AT, Pereira Junio RF, de Neuba L, M, et al (2020) Caranán fiber from *Mauritiella armata* palm tree as novel reinforcement for epoxy composites. *Polymers* 12:2037. <https://doi.org/10.3390/polym12092037>
- Souza FG, De Araújo FF, Orlando EA et al (2022) Characterization of buritirana (*Mauritiella armata*) fruits from the Brazilian Cerrado: biometric and physicochemical attributes, chemical composition and antioxidant and antibacterial potential. *Foods* 11:786. <https://doi.org/10.3390/foods11060786>
- Steinbrecher T, Leubner-Metzger G (2017) The biomechanics of seed germination. *J Exp Bot* 68:765e783. <https://doi.org/10.1093/jxb/erw428>
- Tweddle JC, Dickie JB, Baskin CC, Baskin JM (2003) Ecological aspects of seed desiccation sensitivity. *J Ecol* 91:294–304. <https://doi.org/10.1046/j.1365-2745.2003.00760.x>
- Veloso VHS, Ribeiro LM, Mercadante-Simões MO, Nunes YRF (2016) Cytological aspects of recalcitrance in dormant seeds of *Mauritia flexuosa* (Arecaceae). *Acta Physiol Plant* 38:171. <https://doi.org/10.1007/s11738-016-2194-7>
- Vidal BC (1970) Dichroism in collagen bundles stained with Xylidine-Ponceau 2R. *Ann Histochem* 15:289–296
- Visscher AM, Castillo-Lorenzo E, Toorop PE, Junio Da Silva L, Yeo M, Pritchard HW (2020) Pseudophoenix ekmanii (Arecaceae) seeds at suboptimal temperature show reduced imbibition rates and enhanced expression of genes related to germination inhibition. *Plant Biol J* 22(6):1041–1051. <https://doi.org/10.1111/plb.13156>
- Watson ML (1958) Staining of tissue sections for electron microscopy with heavy metals II. Application of solutions containing lead and barium. *J Biophys Biochem Cytol* 4:727–730
- Weis KG, Polito VS, Labavitch JM (1988) Microfluorometry of pectic materials in the dehiscence zone of almond (*Prunus dulcis* [Mill.] DA Webb) fruits. *J Histochem Cytochem* 36:1037–1041. <https://doi.org/10.1177/36.8.3392393>
- Zona S (2004) Raphides in palm embryos and their systematic distribution. *Ann Bot* 93:415–421. <https://doi.org/10.1093/aob/mch060>

Publisher's Note Springer Nature remains neutral with regard to jurisdictional claims in published maps and institutional affiliations.

Springer Nature or its licensor (e.g. a society or other partner) holds exclusive rights to this article under a publishing agreement with the author(s) or other rightsholder(s); author self-archiving of the accepted manuscript version of this article is solely governed by the terms of such publishing agreement and applicable law.